TURUN YLIOPISTON JULKAISUJA
ANNALES UNIVERSITATIS TURKUENSIS

SARJA - SER. D OSA - TOM. 926

MEDICA - ODONTOLOGICA

CT AND PET/CT HYBRID IMAGING OF CORONARY ARTERY DISEASE

by

Sami Kajander

TURUN YLIOPISTO
UNIVERSITY OF TURKU
Turku 2010

From Turku PET Centre and the Department of Clinical Physiology and Nuclear Medicine, University of Turku, Turku Finland

Supervised by

Professor Juhani Knuuti, MD, PhD
Turku PET Centre
University of Turku
Turku, Finland

Reviewed by

Adjunct Professor Marja Hedman, MD, PhD
Heart Center
Kuopio University Hospital
Kuopio, Finland

and

Professor Stephen Schroeder, MD, PhD
Medizinische Klinik I
Klinik am Eichert
Göppingen, Germany

Dissertation opponent

Professor Pim de Feyter, MD
Department of Cardiology and Radiology
Erasmus Medical Center
Rotterdam, the Netherlands

ISBN 978-951-29-4425-5 (PRINT)
ISBN 978-951-29-4426-2 (PDF)
ISSN 0355-9483
Painosalama Oy – Turku, Finland 2010

With a little help from my friends

ABSTRACT

Sami Kajander

CT AND PET/CT HYBRID IMAGING OF CORONARY ARTERY DISEASE

From Turku PET Centre and Department of Clinical Physiology and Nuclear Medicine,

University of Turku, Turku, Finland

Coronary artery disease (CAD) is a chronic process that evolves over decades and may culminate in myocardial infarction (MI). While invasive coronary angiography (ICA) is still considered the gold standard of imaging CAD, non-invasive assessment of both the vascular anatomy and myocardial perfusion has become an intriguing alternative. In particular, computed tomography (CT) and positron emission tomography (PET) form an attractive combination for such studies. Increased radiation dose is, however, a concern. Our aim in the current thesis was to test novel CT and PET techniques alone and in hybrid setting in the detection and assessment of CAD in clinical patients. Along with diagnostic accuracy, methods for the reduction of the radiation dose was an important target. The study investigating the coronary arteries of patients with atrial fibrillation (AF) showed that CAD may be an important etiology of AF because a high prevalence of CAD was demonstrated within AF patients. In patients with suspected CAD, we demonstrated that a sequential, prospectively ECG-triggered CT technique was applicable to nearly 9/10 clinical patients and the radiation dose was over 60% lower than with spiral CT. To detect the functional significance of obstructive CAD, a novel software for perfusion quantification, Carimas™, showed high reproducibility with ^{15}O-labelled water in PET, supporting feasibility and good clinical accuracy. In a larger cohort of 107 patients with moderate 30-70% pre-test probability of CAD, hybrid PET/CT was shown to be a powerful diagnostic method in the assessment of CAD with diagnostic accuracy comparable to that of invasive angiography and fractional flow reserve (FFR) measurements. A hybrid study may be performed with a reasonable radiation dose in a vast majority of the cases, improving the performance of stand-alone PET and CT angiography, particularly when the absolute quantification of the perfusion is employed.

These results can be applied into clinical practice and will be useful for daily clinical diagnosis of CAD.

Key Words: Coronary Artery Disease, Positron Emission Tomography, Computed Tomography, Hybrid Imaging

TIIVISTELMÄ

Sami Kajander

SEPELVALTIMOTAUDIN KUVANTAMINEN TIETOKONETOMOGRAFIALLA (TT), POSITRONIEMISSIOTOMOGRAFIALLA (PET) JA NIIDEN YHDISTELMÄLLÄ (PET/TT)

Valtakunnallinen PET-keskus, Kliinisen fysiologian ja isotooppilääketieteen oppiaine, Kliininen laitos, Turun Yliopisto

Sepelvaltimotauti on krooninen verisuonten sairaus, joka kehittyy vuosikymmenten aikana ja joka saattaa johtaa sydäninfarktiin. Vaikka perinteinen, kajoava verisuonten varjoainekuvaus (angiografia) onkin yhä tarkin sepelvaltimotaudin kuvantamistapa, on sekä sepelvaltimoiden anatomian että sydänlihaksen verenvirtauksen (perfuusio) kajoamaton arvio yhä useammin sen vaihtoehto. Tällöin erityisesti tietokonetomografian (TT) ja positroniemissiotomografian (PET) yhdistelmä on houkutteleva, mutta tällaisen hybriditutkimuksen potilaalle aiheuttama säderasitus tulee huomioida. Tämän väitöskirjan tavoite oli tutkia uusia TT- ja PET-tekniikoita ja niiden yhdistelmiä sepelvaltimotaudin toteamisessa ja sen vaikeusasteen määrittämisessä kliinisillä potilailla. Diagnostisen tarkkuuden arvioinnin lisäksi päämääränä oli selvittää keinoja vähentää näiden tutkimusten potilaille aiheuttamaa säderasitusta. Tutkimus, jossa TT:n avulla todettiin eteisvärinäpotilailla vertailuryhmää enemmän sepelvaltimotaudin löydöksiä, vahvisti olettamuksen jonka mukaan eteisvärinän syy voi olla sepelvaltimotauti. Todistimme myös, että prospektiivisesti EKG-tahdistettu tietokonetomografia oli tehokas ja helposti toteutettavissa, sillä sitä voitiin käyttää lähes yhdeksällä potilaalla kymmenestä, ja sen käyttö alensi potilaiden sädeannosta yli 60% verrattuna spiraalimenetelmään. Carimas™ –ohjelma osoittautui toistettavaksi ja luotettavaksi sydänlihaksen perfuusion mittaamisessa käytettäessä merkkiaineena ^{15}O –leimattua vettä. Selvitimme myös, että PET:n ja TT:n yhdistelmä on tarkka menetelmä sepelvaltimotaudin arvioimisessa. Menetelmä on erityisen tehokas käytettäessä verenvirtauksen kvantitointia, ja on tällöin tarkkuudeltaan verrattavissa perinteisen varjoainetutkimuksen ja painevaijerimittauksen yhdistelmään.

Tutkimustuloksilla on suuri kliininen merkitys sepelvaltimotaudin diagnostiikassa.

Avainsanat: Sepelvaltimotauti, positroniemissiotomografia, tietokonetomografia, hybridikuvantaminen

TABLE OF CONTENTS

ABBREVIATIONS

BMI	Body mass index
CAD	Coronary artery disease
CHF	Congestive heart failure
CT	X-ray computed tomography
CTA	Computed tomography angiography
DM	Diabetes mellitus
DSCT	Dual source computed tomography
EBCT	Electron beam computed tomography
FFR	Fractional flow reserve
HR	Heart rate
ICA	Invasive coronary angiography
IGT	Impaired glucose tolerance
LAD	Left anterior descending artery
LCX	Left circumflex artery
LM	Left main artery
LV	Left ventricle
MBF	Myocardial blood flow
MDCT	Multi detector computed tomography
MI	Myocardial infarction
MP	Myocardial perfusion
MRI	Magnetic resonance imaging
NPV	Negative predictive value
PET	Positron emission tomography
PET/CT	Hybrid positron emission tomography and computed tomography
PPV	Positive predictive value
RCA	Right coronary artery
ROI	Region of interest
SPECT	Single photon emission computed tomography

LIST OF ORIGINAL PUBLICATIONS

This dissertation is based on the following original publications, which are referred in the text by the corresponding Roman numerals, I-V.

I Kajander S, Ukkonen H, Sipilä H, Teräs M, Knuuti J. Low radiation dose imaging of myocardial perfusion and coronary angiography with a hybrid PET/CT scanner. *Clin Physiol Funct Imaging.* 2009 Jan;29(1):81-8.

II Nucifora G, Schuijf JD, Tops LF, van Werkhoven JM, Kajander S, Jukema JW, Schreur JHM, Heijenbrok MW, Trines SA, Gaemperli O, Turta O, Kaufmann PA, Knuuti J, Schalij MJ, Bax JJ. Prevalence of coronary artery disease assessed by multislice computed tomography coronary angiography in patients with paroxysmal or persistent atrial fibrillation. *Circ Cardiovasc Imaging.* 2009 Mar;2(2):100-6.

III Nesterov SV, Han C, Mäki M, Kajander S, Naum AG, Helenius H, Lisinen I, Ukkonen H, Pietilä M, Joutsiniemi E, Knuuti J. Myocardial perfusion quantitation with 15O-labelled water PET: high reproducibility of the new cardiac analysis software (Carimas™). *Eur J Nucl Med Mol Imaging.* 2009 Oct;36(10):1594-602. Erratum in: *Eur J Nucl Med Mol Imaging.* 2010 Apr;37(4):832.

IV Kajander S, Joutsiniemi E, Saraste M, Pietilä M, Ukkonen H, Saraste A, Sipilä HT, Teräs M, Mäki M, Airaksinen J, Hartiala J, Knuuti J. Cardiac positron emission tomography/computed tomography imaging accurately detects anatomically and functionally significant coronary artery disease. *Circulation;* 2010 Aug 10;122(6):603-13.

V Kajander S, Joutsiniemi E, Saraste M, Pietilä M, Ukkonen H, Saraste A, Sipilä HT, Teräs M, Mäki M, Aalto V, Airaksinen J, Hartiala J, Knuuti J. Clinical value of absolute quantification of myocardial perfusion in coronary artery disease. *Submitted for publication.*

1. INTRODUCTION

Atherosclerosis evolves over a long period of time and may culminate in coronary artery disease (CAD) and, all too often, in myocardial infarction (MI). Evaluation of patients with suspected CAD has been based on non-invasive methods of detecting myocardial ischemia followed by invasive coronary angiography to visualize the presence of possible stenoses. This diagnostic pathway, however, has recently been challenged by the development of coronary multi-detector CT (MDCT), which has emerged as a widely used imaging modality in the non-invasive arsenal of cardiac imaging. As an evolving method, its proper usage is still under discussion and the indications for coronary CT angiography (CTA) are disputed. Despite of this, the number of coronary CTA studies has increased rapidly as improvement in technology has occurred. The ability to non-invasively image coronary arteries, and to obtain important clinical information on the characteristics of CAD constitutes an interesting option to the traditional diagnostic tools (Berman DS, *et al* 2004; Berman DL, *et al* 2006).

Yet, while CTA gives an estimate of the degree of the atherosclerotic burden and may even assess plaques at the risk of rupture, it – like any other *anatomical* imaging modality – is not able to quantify the functional significance of the luminal changes. There is often disparity between the magnitude of the lesions and their effects on myocardial blood supply. Only half of the anatomically significant (usually considered to be >50%) lesions detected with CTA are actually flow-limiting: Meijboom *et al* (2008) reported 49% accuracy of CTA predicting reduced fractional flow reserve (FFR) during invasive angiography (ICA) while Gaemperli *et al* (2007) found that 50% of the lesions found in CTA were linked with impaired perfusion in single photon emission tomography (SPECT).

Since the 1980`s it has been well demonstrated that myocardial perfusion can be evaluated by using positron emission tomography (PET) (Hack, *et al* 1980; Bergmann, *et al* 1984; Knabb, *et al* 1985). Studies have compared image quality between PET and SPECT with significant differences in favor of PET (Yoshinaga *et al* 2006, Bateman, *et al* 2006). When clinical scanners combining PET and CT appeared in the late 1990`s, the idea of combining the methods into a hybrid modality became attractive. First, it was shown that the amount of calcium in coronary walls correlates with impaired coronary perfusion (although the absence of coronary calcifications does not rule out significant CAD) (Schenker, *et al* 2008). After CT technology improved to the current state of allowing visualization of practically all coronary segments, also cardiac PET/CTA became a reality.

The techniques and imaging schemes of cardiac PET/CTA are still under progression. Practical and robust software is needed for optimal assessment of myocardial blood flow (MBF) in PET. However, the greatest attention in CT, in addition to

image quality, is paid for the reduction of radiation dose to the patients. Clinically, the most important issue is a proper patient selection for the study.

It is of vital importance to find the strengths of each imaging modality and to further improve the possible weaknesses. This could make cardiac PET/CT a truly beneficial and clinically valuable method for the diagnostics of CAD, and, in the end, improve patient care.

2. REVIEW OF THE LITERATURE

2.1 Coronary Artery Disease

2.1.1 Definition & Risk Factors

Coronary artery disease (CAD) refers collectively to stenosis, aneurysm, or inappropriate vasomotor behaviour of the coronary arteries usually due to atherosclerosis. A chronic disease of large, medium, and small arteries, atherosclerosis evolves over decades and often culminates in myocardial infarction (MI), reduced cardiac output, or ventricular arrhythmia (American Heart Association 2003-4; Arias, *et al* 2001; Castelli, *et al.* 1986; Kannel, *et al* 1976; Kannel&McGee 1979). With mortality rates of more than 30% at 1 month and 45% at 1 year (Morrow K, *et al.* 1993), MI and its complications are the principle cause of death for patients with CAD. Such dire consequences have stimulated a preventive approach to atherosclerosis that hinges less upon the identification of specific lesions and more upon the recognition of individuals with high risk of lesion development. Atherosclerotic lesion development, the rate of disease progression, and the occurrence of dramatic clinical events closely correlate with inherited and acquired metabolic and behavioural risk factors (Castelli, *et al* 1986; Kannel&McGee 1979; Wilson, *et al* 1998;. Myers, *et al* 1990)

2.1.2 Atrial Fibrillation and CAD

Atrial fibrillation (AF) is the most common sustained cardiac arrhythmia with an estimated prevalence of 0.4% to 1% in the general population (Fuster*, et al* 2006). In addition, the mortality rate of patients with AF is almost twice as high as in patients with normal sinus rhythm. This observation has been attributed to an increased cardiac death rate due to underlying heart disease (Flegel, *et al* 2007; Kannel, *et al* 1983; Krahn, *et al* 1995; Psaty, *et al* 1997) rather than to thromboembolism (Dries, *et al* 1998). CAD is considered to be highly prevalent among patients with AF and may be one of its underlying causes (Lip& Beevers 1995). Furthermore, it has been suggested that AF may be the sole manifestation of CAD (Schoonderwoerd, *et al* 1999). However, the majority of data supporting this association have been derived from studies using the presence of electrocardiographic (ECG) abnormalities and a history of ischemic heart disease to define CAD (Krahn, *et al* 1995; Schoonderwoerd, *et al* 1999, Kannel, *et al* 1982) rather than direct visualization of atherosclerosis. Thus far, only 2 cardiac imaging studies of this topic are available. In these investigations, stress myocardial perfusion single-photon emission computed tomography (SPECT) was applied to evaluate the prevalence of CAD in patients with AF (Abidov, *et al* 2004; Askew, *et al* 2007). In the former paper, Abidov and colleagues showed a

significantly higher prevalence of abnormal myocardial perfusion SPECT findings in AF patients as compared to patients without AF. However, in this study patients with symptoms and known CAD were included. Investigation of an asymptomatic population, as performed by Askew et al, failed to confirm this observation.

2.1.3 Current and Evolving Diagnosis of CAD

Even though we have witnessed a significant improvement in the prevention and management of CAD and its devastating consequences, it still remains highly prevalent and represents a healthcare burden: symptomatic atherosclerosis is the second leading cause of death by the age of 65 years (Arias, *et al* 2003). To enhance earlier diagnosis, an expansion and refinement of non-invasive imaging methods has occurred, and an intense debate regarding the strengths and weaknesses of competing imaging technologies and their appropriate clinical use is still on-going. The introduction and dissemination of new technology provides the potential for enhancing and expanding our understanding of the pathogenesis and natural history of the disease (eg, atherosclerosis and myocardial dysfunction) and hopefully extend our treatment options while providing a tool for monitoring therapeutic responses (Einstein, *et al* 2007).

The detection of ischemia is based on either reduction of perfusion or induction of ischemic wall motion abnormalities during exercise or pharmacological stress. The most well-established stress imaging techniques include stress echocardiography and SPECT. Both may be performed with either exercise stress or pharmacological stress. Novel stress imaging techniques include stress magnetic resonance imaging (MRI), PET and combined approaches. Stress imaging techniques have several advantages over the conventional exercise ECG test because they offer more sensitive and specific diagnostic performance (Fox, *et al* 2006), the ability to quantify and localize areas of ischemia, the ability to provide diagnostic information in the presence of resting ECG abnormalities or in cases in which the patient is not able to exercise.

2.2 MDCT Imaging of CAD

2.2.1 CT technology

2.2.1.1 Early Development

A tomographic scanner rotates to produce spatially consecutive, parallel image sections. In CT, a computer stores a large amount of x-ray attenuation values of an object, thus making it possible to determine the spatial relationship of the radiation absorbing structures within it. A computed tomogram consists of a matrix of attenuation values presented in shades of grey, thereby creating a spatial

image of the scanned object. After Cormack`s initial work on image reconstruction from projections (Cormack 1964a, Cormack 1964b), the first modern CT scanner was produced in the early 1970`s by Hounsfield working for EMI Ltd. in England. The device, although requiring 9 days to complete the acquisition of the data, revolutionized medical imaging (Hounsfield 1973; Ambrose 1973). During the next decade, gradual but important steps were taken to further improve the device. Many of them were enhanced by the rapid development of the electronics, thus making it possible to image faster, which in turn was necessary to image moving organs and larger volumes of the body. In addition, the deployment of iodine-containing contrast media improved contrast resolution and made it possible to image blood vessels.

2.2.1.2 Electron Beam CT

Imaging of the heart was an early but ambitious target for CT imaging. During the late 1970`s it seemed clear that mechanically rotating gantry could not freeze cardiac motion, and that an alternative solution should be found. In 1978, a device with an electron beam scanning on tungsten rings was proposed, creating an electron beam CT (EBCT) (Boyd 1979). In an EBCT scanner, an electron gun produces a beam of electrons that are expanded, refocused, bent and rotated to form multi-slice images through computer control. The first devices were introduced commercially in 1984 as cardiac scanners, were updated in 1988 as whole body tomographs (Boyd, *et al* 1987), but never gained wide acceptance. Although still the fastest CT-device (with temporal resolution of up to 33 msec) and the only CT technology to compete with invasive angiography in speed, problems with high costs and suboptimal contrast/noise hindered the development and sales of EBCT scanners. Only about 300 examples were built.

2.2.1.3 Spiral and Multi Detector CT

The breakthrough invention for CT, however, was the development of spiral imaging, enabling the scanner`s detector ring to rotate continuously and to produce a helical – or spiral – data set of the scanned object. In this technology, slip rings transferred power and data to and from a rotating gantry. Spiral imaging eliminated the inter-scan delay of the previous step-scan techniques and allowed faster exams. After single-detector spiral imagers, multi-detector CT (MDCT) technology was introduced by the late 1990`s by several manufacturers. In MDCT, several detector rows are set parallel along Z-axis, allowing simultaneous collection of data from a large volume. After initial 2- and 4-slice configurations, 8-, and 16-row devices soon followed with faster rotation times, thinner slices and, thus, better image quality. In 2005, 64-row – or section – MDCT become available, further reducing imaging time and allowing reconstruction of extremely thin slices down to 0.5 mm.

2.2.1.4 Current and Future Developments

Since then, fast 256- and 320-row configurations have reached marketplace. The latter, introduced by the Japanese company Toshiba in 2007, offers the advantage of imaging larger structures, e.g. human heart, during one gantry rotation. In addition, CT perfusion is enhanced because the field of view in Z-axis is longer (Choi, *et al* 2009). One manufacturer (Siemens) has opted for developing and producing a device with two separate x-ray tubes and detectors, offering improved time resolution and thus less motion artefacts in moving targets. In this type of device, it is possible to use a different energy in each tube resulting in better contrast (Rogalla, *et al* 2009). General Electric (GE), on the other hand, has a scanner producing energy sensitive images using a single tube system in which the electric current is rapidly changed between two levels. A new detector material (gemstone) may offer better contrast resolution whereas iterative reconstruction is employed for less image noise. In addition, future directions of CT development include analytic reconstruction, local or interior reconstruction, flat-panel based CT, multi-source CT, novel scanning modes, artefact reduction, modality fusion, and phase-contrast CT (Wang, *et al* 2008).

2.2.1.5 Image Processing

Along with the improvement in mechanics and electronics, advances in visualization techniques and data processing have been and continue to be mandatory to handle the information (Rubin 2005). While a single row scanner produced about 20-40 MB of data per a whole body scan, this amount rose to more than 700 MB by the year 2005. This data explosion necessitated several image processing techniques such as Maximal Intensity Projection (MIP), Multiplanar Reformation (MPR) and Volume Rendering (VR) (Choi, *et al* 2009). These techniques have allowed the radiologist – or radiographer – to efficiently handle and visualize a large data volume without the need to film each image.

2.2.2 Imaging CAD with MDCT

2.2.2.1 Comparison to Conventional Coronary Angiography

Currently, modern MDCT offers a tool for successful imaging of fast moving small structures such as coronary arteries. Images can be ECG gated or triggered for freezing the motion, acquisition is fast enough for covering the heart during a few heart beats; new technologies allow for fast gantry rotation with narrow collimation and with good image quality (Budoff, *et al* 2006, Stein, *et al* 2006; Blue Cross and Blue Shield Association 2006).

The use of intravenous iodinated contrast enables direct visualization of coronary stenoses with MDCT. At present, a large number of studies performed with 64-section MDCT technology have been published. At least 6 meta-analyses have shown that

the negative predictive value of the method is excellent, close to 100%, suggesting that MDCT can reliably rule out the presence of hemodynamically significant CAD. Positive predictive value, however, has been less impressive (Vanhoenacker, *et al* 2007; Janne d´Othee, *et al* 2008; Sun, *et al* 2007; Abdulla, *et al* 2007; Di Tanna, *et al* 2008; Mowatt, *et al* 2008). In most cases, this is due to overestimation of detected stenoses in MDCT. Of the two multi-centre trials published, the other was consistent with the results of meta-analyses (Meijboom, *et al* 2008) but the other showed only moderate negative predictive value for CAD (Miller, *et al* 2009).

Even with 64-section MDCT, 3-11% of coronary artery segments cannot be evaluated (Raff, *et al* 2005; Ferencik, *et al* 2006; Wintersperger, *et al* 2006; Pannu, *et al* 2006; Leschka, *et al* 2005; Leschka, *et al* 2006; Pugliese, *et al* 2006). Interestingly, of the coronary artery segments that were included in 64-MDCT studies, the accuracy for detecting stenoses depended highly on image artifacts. False-positive and false-negative interpretations were attributed to image artifacts in 91% (Raff, *et al* 2005) to 100% (Leschka, *et al* 2005), the major cause being the presence of calcifications. Less frequent causes of degraded image quality were motion artifacts and obesity, the latter resulting in a poor contrast-to-noise ratio.

Most studies comparing the diagnostic performance of coronary MDCT with invasive angiography have suffered from verification bias; they have investigated populations requiring invasive approach (high risk patients) thus differing from the general population. Recently, the clinical performance in non-selected patient populations has also been investigated: Grosse, *et al* (2007) found a sensitivity, specificity, positive predictive value, and negative predictive value of 87%, 99%, 98%, and 95%, respectively, in segment-based analysis. In patient-based analysis, the analysis demonstrated an excellent negative predictive value of 91%.

2.2.2.2 Comparison with MRI

When comparing MDCT angiography with another non-invasive imaging modality, MRI, MDCT has significantly higher accuracy for the detection of coronary artery stenosis (Dewey, *et al* 2006; Schuijf, *et al* 2006).

2.2.2.3 Clinical Appropriateness

A recent scientific statement of the American Heart Association concluded that coronary CTA may be clinically useful and may be reasonable for the assessment of symptomatic patients with suspected CAD (evidence class IIA, level of evidence: B) (Budoff, *et al* 2006). Furthermore, the American College of Radiology has issued a similar practice guideline including appropriateness criteria for the performance of cardiac CT (Jacobs, *et al* 2006).

2.2.2.4 Radiation Dose of Cardiac MDCT

Radiation dose has become a major safety issue in cardiac imaging. The patient dose of cardiac MDCT is considerable: radiation due to a coronary CT angiogram on an industry standard 64-section MDCT scanner is higher than with older versions such as 16-slice devices. This issue, together with the increased number of the studies performed, the dose received by the population has grown and is expected to further increase (Einstein *et al.* 2007; Nickoloff & Alderson 2007; Paul & Abada 2007). This is against the ALARA (As Low as Reasonably Achievable) philosophy of using radiation, and has enhanced efforts to reduce radiation dose with novel imaging technologies.

The mean radiation dose in 64-section MDCT cardiac studies has been estimated to be 15.2 mSv for males and 21.4 mSv for females (de Feyter, *et al* 2007). However, the true patient doses vary in daily practice and individual doses may increase up to 40 mSv (Paul & Abada 2007). The most recent survey (Hausleiter, *et al* 2009) showed that the differences between imaging centers and CT systems still exist. Even though the median dose was 12 mSv, the dose varied between 5 and 35 mSv. The employment of novel dose saving protocols has resulted in a dose reduction of 53% in a cohort of 15 hospitals that have used new techniques (Raff, *et al* 2009).

Breast, esophagus and heart have been recorded to have the highest absorbed organ doses. Of particular concern is the female breast, which may receive a dose up to 10-30 times higher than received in mammography screening (Nickoloff & Alderson 2007). In fact, the lifetime risk for breast or lung cancer in girls and young women undergoing a single ECG-gated CT angiography may range from 1.7% to 5.5% (Hurwitz, *et al* 2007). In comparison, diagnostic invasive coronary angiography has a mean effective radiation dose of 7 mSv but has an extremely wide variation between 2.3 and 22.7 mSv. In nuclear perfusion imaging with SPECT, the mean effective radiation dose varies according to the tracer and protocol, being higher with Thallium (~15–20 mSv) than with Technetium-based tracers (~7-11 mSv). Radiation dose data from various cardiac imaging methods is presented in **Figure 1** (reprinted with permission, Einstein, *et al* 2007).

~

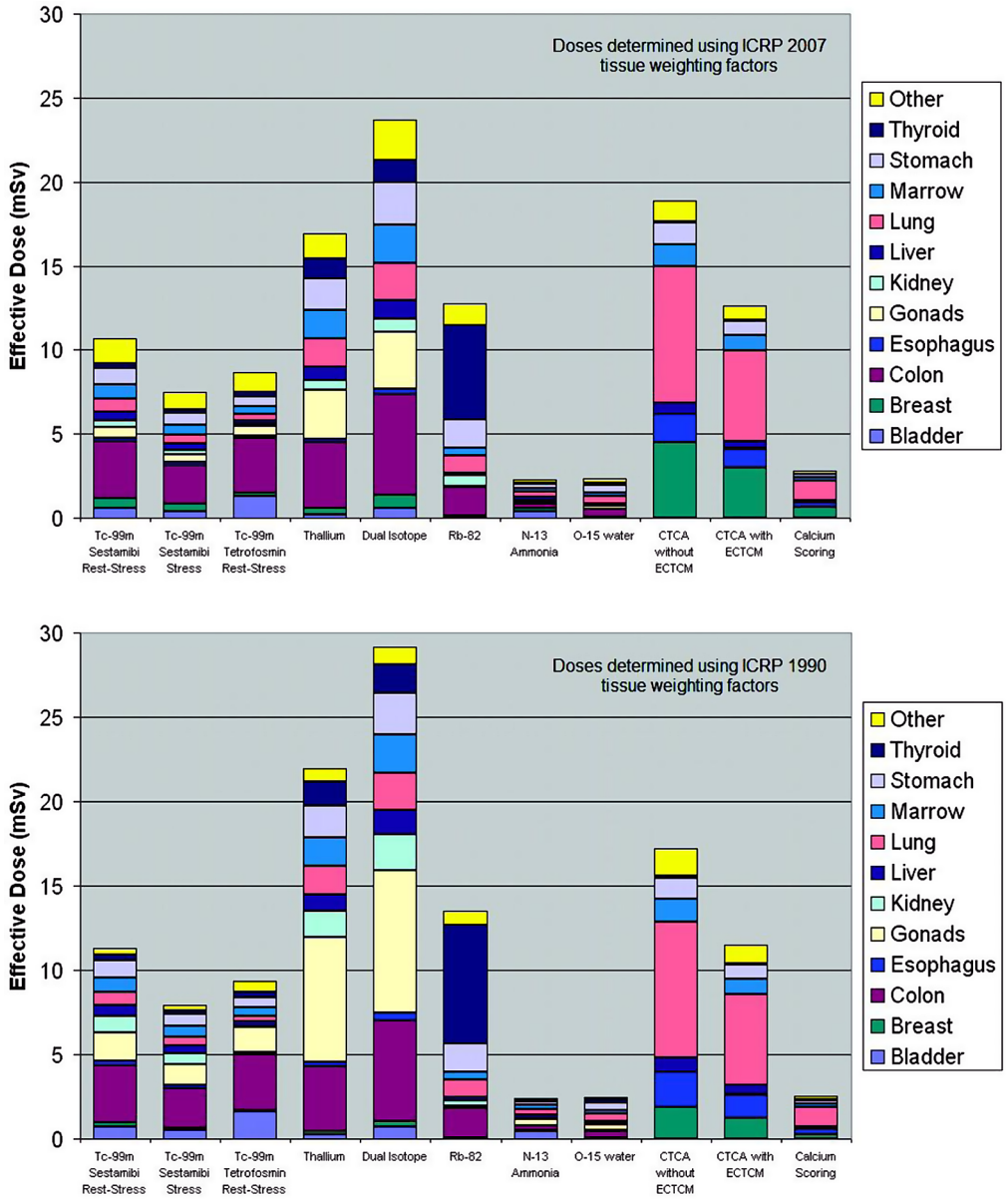

Fig. 1.

2.2.3 Strategies for Radiation Dose Reduction in Cardiac MDCT

2.2.3.1 Patient Selection

The most important means to avoid unnecessary radiation are, of course, proper patient selection and preparation. Proper clinical indications must be met and contraindications to the study, such as a non-sinus rhythm, taken into consideration. Massive coronary calcifications and tissue motion deteriorate image quality (Mir-

Akbari, *et al* 2009) and it has been stipulated that patients with very high calcium scores should be omitted from CTA in favour of other methods. Recently, it has been stated that instead of applying a strict upper limit of coronary calcifications, possible denial of the CTA should be considered individually – but on the basis of the calcification score (Hecht & Bhatti 2008).

2.2.3.2 Traditional Methods of Dose Reduction

The conventional methods to decrease dose are reducing tube current and voltage and increasing the pitch. These methods are widely used but always compromise image quality. However, it is advisable to use a lower (100 kV) tube voltage (Leschka, *et al* 2008) or even 80 kV (Abada, *et al* 2006) in slim individuals. Anatomy based current modulation (either real time or scout image based) depends on tissue attenuation; radiation increases with increasing amount of tissue. A more sophisticated method, ECG-dependent X-ray tube current modulation, reduces current only at phases outside the critical time window between end systole and end diastole. This method reduces the tube current by up to 80% during systole while delivering the full dose during diastole, resulting in a 30%–50% reduction in the effective radiation exposure. If the width of the time window for maximal mAs may be adjusted, dose will be further reduced (Kalender, *et al* 1999; Morin, *et al* 2003; Prinak, *et al* 2006; Fei, *et al* 2007).

2.2.3.3 Prospective ECG-triggering

Another new method to reduce radiation dose is called sequential acquisition, or "step and shoot". It uses axial CT images in the context of contrast-enhanced, thin slice MDCT cardiac imaging. In contrast to normally used spiral protocols with retrospective ECG-gating, it utilizes prospective triggering with a pre-determined scan window that may be widened up to include a series of adjacent phases. The image data are post-processed after the scan to reconstruct only this particular portion of the ECG-cycle. Contrary to spiral imaging, in which acquisition takes place during the table motion, tube current is on and the data collected only between sequential table movements. Typically, this takes place during every other heart beat. It also means that the pitch is always 1 with a pre-decided overlap between the image stacks. A normal sized heart can be scanned in 3 to 4 acquisitions during 5 to 7 heart beats with a current standard 4 cm system. Standard 64-section hardware may be used. Thus, step and shoot imaging is essentially a modification of traditional axial imaging adapted to a wide MDCT detector and it may be coupled to DSCT hardware, too.

Sequential imaging may offer diagnostic CTA at doses as low as 1-2 mSv (Hsieh, *et al* 2006; Herzog, *et al* 2008; Husmann, *et al* 2008; Scheffel *et al* 2008; Schoenhagen, *et al* 2008; Herzog *et al* 2009; Pontone, *et al* 2009) without sacrificing general image quality. The main limitations of the method are the lack of information about left ventricular function (as most phases of the cardiac cycle are omitted), the relative

sensitivity to heart rate variability, and the inability to image at high heart rates due to the short reconstruction time available at such rates. Heavy calcifications deteriorate image quality as with retrospective gating (Husmann, *et al.* 2008, Scheffel, *et al* 2008, Stolzmann, *et al* 2008).

2.2.3.4 New Hardware Development

The most recent innovations in CT dose containment largely depend on new technical advances and the need for new hardware such as wide 256- or 320-slice detector arrays. With DSCT scanners, good image quality may be achieved with reduced radiation dose: multiple sources enable increased pitch of a scan, and correspondingly a lower dose. These machines may improve image quality to dose ratio especially at higher heart rates (McCollough, *et al* 2007; Stolzmann, *et al* 2008). A high-pitch mode of the DSCT has also been introduced with promising preliminary results for both the diagnostic accuracy and lower radiation dose (Leschka, *et al* 2009).

2.3 Myocardial Perfusion

While CT gives an estimate of the degree of atherosclerotic burden and may even reveal some plaques at rupture risk, it fails to quantify vascular endothelial health, vascular reactivity and the flow limiting consequences of the luminal changes. Therefore, it is difficult to evaluate the effects of a vascular lesion on myocardial blood supply. Only half of the anatomically significant lesions detected in CTA are flow-limiting; Meijboom. *et al* (2008) reported 49% accuracy of CTA predicting reduced fractional flow reserve (FFR) during invasive angiography (ICA) and Gaemperli, *et al* (2007) showed that 50% of the lesions in CTA were associated with perfusion defects in SPECT. The accuracy of 64-section coronary CTA was compared with that of technetium 99m tetrofosmin SPECT myocardial perfusion for functionally significant CAD. Sensitivity, specificity, negative predictive value and positive predictive value of CTA against any perfusion defects were 75%, 90%, 93% and 68%, respectively, per patient.

Treatment of the lesions is based on ischemia correlating to subjective symptoms. Thus, functional assessment is needed particularly when evaluating intermediate lesions in CTA and the therapy of stenoses without functional effects can be deferred. The measurement of FFR during ICA has been used as a gate keeper for angioplasty, but too often the treatment decisions are done on the basis of vessel anatomy (Pijls, *et al* 2004; Botman, *et al* 2004; Berger, *et al* 2005; Tonino, *et al* 2009).

2.3.1 Assessment of Myocardial Ischemia

Traditionally, diagnosis of CAD has been based on detecting myocardial ischemia. Ischemia can be documented by symptom-limited exercise test and non-invasive

imaging of myocardial perfusion. Assessment of myocardial perfusion is the standard method of detecting ischemia and thus determining the functional consequences of impaired blood flow in the epicardial arteries. In cases of seriously impaired myocardial perfusion, invasive angiography can be performed to evaluate the need for vascular interventions.

2.3.1.1 Assessment of Myocardial Ischemia with SPECT

SPECT perfusion test is an established diagnostic method which provides more sensitive and specific prediction of the presence of CAD than exercise ECG. Reported sensitivity and specificity of exercise SPECT when compared against invasive angiography ranges between 85–90% and 70–75%, respectively (Fox, *et al* 2006). SPECT has been successfully performed for over 30 years, and its diagnostic and prognostic value is confirmed by extensive literature. Over the years, advances have been made to improve image quality and shorten acquisition protocols (Bateman, *et al* 2009; Heller, *et al* 2009). Despite this progress, SPECT still suffers from several limitations. It frequently underestimates the degree of ischemia and, in particular, the presence of multivessel disease because the analysis is either relative (qualitative) or, at best, semi-quantitative. The stress protocols are still rather time-consuming (up to 2.5 – 4 hrs). Attenuation artefacts are common and tracer activity in liver and gut is considerable. (Heller, *et al* 2009).

2.3.1.2 Assessment of Myocardial Ischemia with MRI

Cardiac MRI with pharmacological stress can be used to detect myocardial ischemia. Ischemia may be detected by screening for wall motion abnormalities induced by dobutamine infusion or perfusion abnormalities induced by adenosine. Cardiac MRI has rather recently been applied in clinical practice and therefore less data have been published of it than of other established noninvasive imaging techniques (Fox, *et al* 2006).

A recent meta-analysis showed that stress-induced wall motion abnormalities in MRI have sensitivity of 83% and specificity of 86% in patient-based analysis. Furthermore, perfusion imaging demonstrated 91% sensitivity and 81% specificity (Nandalur, *et al* 2007). One multicenter trial has been published of the performance of stress perfusion MRI in the detection of CAD with 85% sensitivity and 67% specificity (Schwitter, *et al* 2008).

2.3.1.3 Assessment of Myocardial Ischemia with Stress Echocardiography

Stress echocardiography is an established diagnostic test and is more accurate than exercise ECG test in the detection of ischaemia. Physical exercise is usually performed by bicycle ergometer but pharmacological stress with dobutamine and less frequently dipyridamole can also be used. The technique requires adequate training and experience since it is more user dependent than other imaging

techniques. Pooled sensitivity and specificity of exercise echocardiography are reported as 80–85% and 84–86%, respectively (Fox, *et al* 2006).

2.4 PET Imaging and Myocardial Perfusion

2.4.1 Basics of PET

PET is based on nuclear imaging with short-lived radioactive isotopes such as ^{18}F, ^{11}C and ^{15}O. These radionuclides, which have an excess of protons (thus having a nuclear inbalance), can be labeled with a range of either natural substrates, substrate analogues or pharmaceuticals, enabling quantitative, non-invasive measurements of physiological and biochemical processes in living tissue. After (usually intravenous) administration of the radioactive compound, the radioisotope reaches a stable state thus converting a proton into a neutron, and loses an excess positron. After traveling a short distance and losing some of its energy, the positron collides with an electron to produce two gamma quants of 511 kilo-electron volt (keV) energy in a process called annihilation.

A clinical PET scanner consists of detectors arranged as a ring around the patient. The detectors detect the simultaneous occurrence of two high-energy photons travelling into opposite directions, record the data and send it to a computer for tomographic image reconstruction.

2.4.2 Imaging of Myocardial Perfusion with PET

Since the 1980`s, many studies have demonstrated that myocardial perfusion may be evaluated using PET (Hack, *et al* 1980; Bergmann, *et al* 1984; Knabb, *et al* 1985). As compared to SPECT, PET has several advantages. Image quality is superior due to the higher energy level of PET radiopharmaceuticals (511 vs. 140 keV for the most common SPECT tracer technetium) leading to higher spatial resolution and less scatter. Attenuation correction is routinely used in PET thus reducing attenuation artefact (Heller, *et al* 2009). At least two studies have compared image quality between PET and SPECT with significant differences in favor of PET (Yoshinaga *et al* 2006; Bateman, *et al* 2006).

The diagnostic accuracy of PET is high. A recent meta-analysis demonstrated good overall (92% sensitivity, 85% specificity) and coronary territory-based (81% sensitivity, 87% specificity) accuracy in PET (Nandalur *et al*, 2008). A similar study with solely PET/CT method showed sensitivity of 93% and specificity of 83% (Sampson, *et al* 2007). In a direct comparison between SPECT and PET, the ability of the latter to identify multi-vessel ischemia was significantly better (74% vs 41%) (Bateman, *et al* 2006). With both methods, however, the visualization of just small or relative differences in MBF may lead to underestimation of CAD. On the other hand, quantification of the flow is likely to increase the accuracy of the technique,

especially in the assessment of the severity of multi-vessel disease. Furthermore, quantification allows the detection of myocardial perfusion abnormalities not caused by CAD – such as microvascular disease and endothelial dysfunction (Knuuti, *et al* 2009a; Knuuti 2009b).

A typical radiation dose for a patient to be caused by a PET study is fairly modest and less than by using SPECT. The dose from a rest-stress PET perfusion study is estimated to be 2.2-2.5 mSv for ^{15}O-water and ^{13}N-ammonia but higher (3-13.5 mSv) for ^{82}Rb (Einstein, *et al* 2007).

2.4.3 The Techniques for Quantification of Myocardial Perfusion

There are two main determinants that define the potential of an imaging technique for quantification of myocardial perfusion. The properties of the *imaging device* define the accuracy and robustness of the quantified signal. The other determinant is the choice and characteristics of the *tracer* itself.

Quantification of the tissue tracer concentration is a feature typical to PET. ^{15}O-water and ^{13}N-ammonia are the tracers most widely used for the quantification of myocardial perfusion, Both tracers` kinetic models are well validated in animals against the radiolabeled microsphere method over a wide flow range (Iida, *et al* 1988; Hutchins, *et al* 1990) and are comparable in quantifying perfusion (Bol, *et al* 1993). Absolute quantification of myocardial perfusion in PET is performed by using the tracer kinetic method, which is based on measuring the in vivo kinetics of a tracer concentration during dynamic acquisition, and this analysis can be done in the standard segmentation (Cerqueira, *et al* 2002).

2.4.3.1 Quantification of Myocardial Perfusion with ^{13}N-ammonia

^{13}N-ammonia is extracted from blood with a reasonably high extraction factor. The extraction is, however, inversely related to the perfusion (Knuuti, *et al* 2009a). A three-compartment model has been for calculation of perfusion (Hutchins, *et al* 1990; Muzik, *et al* 1993) and the perfusion is calculated from the tracer`s uptake by myocardium. With ^{13}N-ammonia, quantification of myocardial flow has been proven clinically useful in patients and controls (Muzik, *et al* 1998) and in detecting early vascular pathology before macroanatomical changes occur (Dayanikli, *et al* 1994).

2.4.3.2 Quantification of Myocardial Perfusion with ^{15}O-water

^{15}O-H_2O is an attractive tracer for assessing tissue perfusion. It is metabolically and chemically inert, freely diffusible and may thus be assessed with a single-compartment model for the calculcation of MBF. It has a short half-life (123 seconds) thus allowing serial measurements in a short time span. ^{15}O-H_2O is relatively easily produced in a small cyclotron, may be administered intravenously

and has been validated for quantitative measurement of the regional perfusion (ml/g/min) of myocardium (Iida, *et al* 1988). Unlike when using ^{13}N-ammonia, quantification of MP with ^{15}O-H_2O is estimated on the basis of the tracer´s washout from the myocardium. The most important difference between ^{15}O-H_2O and other perfusion tracers is the linear relationship between absolute myocardial perfusion and tracer behavior. With other tracers, the extraction of the tracer is reduced with increased perfusion thus causing underestimation of the actual flow. This must be corrected with a mathematical model using specific equations and a correction factor which may be difficult and cause error and noise to the images (Knuuti, *et al* 2009a). Such corrections are not needed when ^{15}O-H_2O is used.

Already in the mid 1990`s, MBF values with ^{15}O-H_2O PET were shown to reflect properties of both healthy myocardium and tissue affected by coronary stenoses (Uren, *et al* 1994). In addition, it has been shown to exhibit closer correlation with the invasive functional parameter FFR than invasive angiography (De Bruyne, *et al* 1994). It has been shown with ^{15}O-H_2O PET that even early borderline hypertension may impair coronary flow reserve, CFR, a parameter reflecting the relationship between MBF in stress and in rest (Laine *et al* 1998).

Although ^{15}O-H_2O PET allows absolute non-invasive quantification of both global and regional myocardial perfusion (Kaufmann, *et al* 1999), most of the PET studies are still focused on relative perfusion analysis in patients with CAD. This is basically due to the complexity of required acquisition and analysis protocols (Lodge, *et al* 2007). The studies with absolute quantification typically assess cardiac perfusion on the global level only, and usually focus on either on the effect of specific risk factors on early coronary dysfunction, or on patients with other cardiovascular diseases such as familial combined hyperlipidemia (Kaufmann, *et al* 1999; Laine, *et al* 1998, Pitkänen, *et al* 1999). Therefore, large studies demonstrating the value of absolute quantification on the detection of CAD, as well as guiding the therapy, are lacking.

2.4.3.3 Other Tracers for Quantification of MP

The most widely used cardiac PET perfusion tracer in clinical use is ^{82}Rb. It may be produced with a column generator and thus at sites lacking a cyclotron providing an important advantage. Despite the non-linear kinetics of the tracer (Herrero, *et al* 1990), studies performed with ^{82}Rb indicate that measurements of the MP are possible and feasible (Parkash, *et al* 2004). They have been shown to be accurate at least with low MBF`s (El Fakhri, *et al* 2009) in patients and controls. Other potential perfusion tracers include new, ^{18}Fluorine based (Madar, *et al* 2006; Huisman, *et al* 2008) and ^{68}Ga-labeled (Plössl, *et al* 2008) compounds.

2.4.4 Interpretation of Absolute Myocardial Perfusion Results

Myocardial blood flow at rest is normally between 0.6 and 1 mL/g/min (Pandit-Taskar, *et al* 2007). When myocardial oxygen demand increases in stress, the coronaries dilate and MBF increases by threefold to fivefold. In regarding to perfusion reserve, values above 2.5-2.7 have been considered normal (Muzik, *et al* 1998). Little clinical data is available about normal and abnormal absolute perfusion values, however. Muzik and colleagues (1998), by using ^{13}N-ammonia, found the optimal cutoff value at 1.52 mL/g/min to separate ischemic from non-ischemic myocardial regions. However, studies performed with ^{82}Rb have suggested lower (Anagnostopoulos C, *et al* 2008) and those obtained with ^{15}O-H_2O higher (Uren, *et al* 1994) cutoff values. Considering the different patient populations, it is clear that more clinical studies are needed to determine the line between normal and abnormal absolute MBF.

2.5 Hybrid Imaging with PET/CT

The introduction of hybrid PET/CT devices in the late 1990`s (Beyer, *et al* 2000; Townsend, *et al* 2002) added a major dimension to the utility of PET. The integration of PET and CT provides an opportunity to provide information of both function and anatomy in a single session exam, adding the full power of PET to the excellent spatial resolution of CT. The new scanners routinely employ industry standard CT quality (at least 64 detector rows) with all the modern PET camera capabilities. Comprehensive non-invasive evaluation of CAD may be obtained in a single session, thus obviating the need for repeated visits and possibly delayed diagnosis.

As stated above, both CT and PET are capable of excluding CAD with good or excellent accuracy. However, in clinical patient populations, only exclusion of the disease is seldom enough; rather, the imaging method needs to accurately assess the significance of the atherosclerotic lesions seen. It is evident that CT (being primarily an anatomical modality) and PET (with the capability to assess tissue metabolism and blood flow) assess a pathological condition from different aspects. By fusing CT and PET data, the location, severity and even composition of the lesions can be detected and their functional significance evaluated (Di Carli *et al* 2007; Di Carli & Hachamovitch 2007; Knuuti 2009b).

CTA provides excellent diagnostic sensitivity for stenoses especially in the proximal and mid segments (>1.5 mm in diameter) of the main coronary arteries. Although the latest CT scanner technology has substantially reduced the number of non-evaluable coronary segments, spatial resolution is still relatively limited when compared to invasive angiography, and worse in distal segments of the coronary vessels compared with the proximal ones (Kaufmann & DiCarli 2009). This limitation can be partly offset by the physiological information obtained with PET that is

generally not affected by the location of coronary stenoses. More importantly, the need for revascularization is based on significant myocardial ischemia associated to clinical symptoms. Stress perfusion information provides valuable clinical information regarding the physiological significance of the anatomic stenoses. This appears to be true in a wide spectrum of CAD prevalence, including low-risk populations (Husmann, *et al* 2008). Although there are often several anatomically significant lesions present, only one of them may be functionally relevant. By using hybrid imaging, these culprit lesions may be accurately assessed.

Thus, hybrid imaging will probably become an important tool for the diagnosis of CAD. The value of coronary PET/CT lies far beyond the simple addition of a further diagnostic test as it allows accurate topographic anatomic association of perfusion defects (Bax, *et al* 2007; Di Carli & Dorbala 2007; Knuuti 2009b).

3. OBJECTIVES OF THE STUDY

The purpose of the present study was to evaluate MDCT and hybrid PET/CT imaging in the diagnosis of CAD. Specific attention was appointed to radiation dose of these studies. The detailed aims were as follows:

1. To investigate the feasibility, image quality and radiation dose of prospectively ECG-triggered sequential CT in the setting of hybrid PET/CT (Study I).

2. To study the prevalence of CAD among patients with paroxysmal or persistent AF and without history of CAD by using multi-detector computed tomography (MDCT) (Study II).

3. To assess the reproducibility of quantification of myocardial perfusion by using Carimas™ (Cardiac Image Analysis System) software package with ^{15}O-H_2O (Study III).

4. To evaluate the value of hybrid PET/CT against ICA and FFR in the diagnosis of CAD (Study IV).

5. To determine the clinical value of absolute quantification of MBF in the diagnosis of CAD (study V).

4. MATERIALS AND METHODS

4.1 Study Design

The study consists of five sub-studies (I-V) that were carried out during 2007-2009. The aim of the study was to evaluate the value of novel imaging methods for non-invasive assessment of CAD in clinical patients. In particular, methods for reducing radiation to the patients and the use of hybrid imaging (PET/CT) for the diagnosis of CAD were of special interest.

Study I was aimed at evaluating the methods for radiation dose reduction in the context of hybrid PET/CT imaging. It consists of two parts. In the first part of the study, a standard spiral and a sequential, prospectively triggered MDCT protocol were compared by the means of image quality and radiation dose. In the second part, we tested whether the sequential imaging protocol is feasible in a larger series of patients. Study II investigates the prevalence of CAD among patients with paroxysmal or persistent AF without a history of CAD. The presence and extent of coronary lesions was evaluated by using MDCT. Study III investigates the properties and feasibility of an in-house developed new software (Carimas™) for the assessment of myocardial perfusion with PET imaging. Study IV was performed by using hybrid PET/CT in a clinical setting. In this study, dose-saving techniques and Carimas software were under special interest. Finally, study V investigated hybrid PET/CT more deeply by evaluating the clinical value of absolute quantification of myocardial blood flow.

4.2 Subjects

Overall, the studies consisted of 544 subjects (396 patients in studies I-V and 148 control patients in Study II). The number of the subjects, according to the study, are shown in Table 1.

Table 1.

Study	N	Patients/ Controls
Study I	10+10+61	81/0
Study II	298	150/148
Study III	10+48	58/0
Study IV	107	107/0
Study V	107	107/0

Patient populations of Studies IV-V are identical.

The first part of Study I included 20 consecutive patients (12 females and 8 males) assigned for cardiac CT angiography according to clinical criteria. First, 10 patients were imaged using a conventional spiral acquisition. The results were compared to those of the following 10 patients performed with a sequential, prospectively ECG-triggered mode. In the second part of the study, 62 patients with suspected CAD, and who were scheduled for hybrid cardiac PET/CT, were enrolled. Exclusion criteria for both of the studies were AF, iodine allergy, unstable angina, severely impaired renal function, 2nd or 3rd degree AV-block, congestive heart failure (CHF) (NYHA IV), symptomatic asthma and pregnancy. One patient was omitted from the final analysis because MDCT acquisition failed due to injection pump malfunction. Thus, final study population of the second part consisted of 61 patients.

In Study II, MDCT was performed in 150 patients with AF (aged 61±11 years, 67% male, 58% asymptomatic for CAD) with predominantly low (59%) or intermediate (25%) pre-test likelihood of CAD. A population of 148 patients without history of AF, similar to the AF group regarding age, gender, cardiac symptoms and pre-test likelihood for CAD, served as a control group.

In the first part of Study III, we analyzed 20 randomly selected ^{15}O-H_2O PET scans from 10 subjects (one "rest" and one "stress" from each patient) with a history of chest pain and 30-70% pre-test likelihood of CAD. In the second (clinical) part of the study, the accuracy of ^{15}O-H_2O perfusion imaging was assessed in 48 consecutive symptomatic patients referred for ICA because of suspected CAD.

For Studies IV and V, we prospectively enrolled 107 consecutive out-patients (64 males and 43 females) with a history of stable chest pain and 30-70% pre-test likelihood of CAD after the analysis of the risk factors and the exercise test. This group included the 61 subjects of the second phase of study I and the 48 patients of the clinical part of study III. Exclusion criteria were AF, iodine allergy, unstable angina, severely impaired renal function, 2nd or 3rd degree AV-block, CHF (NYHA IV), symptomatic asthma and pregnancy. Patients with previously documented CAD or myocardial infarction were not eligible.

The characteristics of the patients in Studies IV and V are exhibited in **Table 2**.

Table 2. Patient characteristics (N=107) of studies IV and V:

Gender (M/F)	**64/43**
Mean age (Y)	**63.6 ± 7.0 (range, 49 - 80)**
Weight (kg)	**77.9 ± 17.8 (range, 50 - 113)**
BMI	**26.6 ± 3.9 (range, 18.4 - 39.1)**
Risk factors for CAD	**#positive**
Family history	48 (45%)
Diabetes	9 IGT (8%)/15 DM type II (14%)
Hypertension	44 (41%)
Hypercholesterolemia	54 (50%)
Smoking or ex-smoking	28 (26%)
Exercise test	90 (84%)
Medication	
Statins	54 (50%)
Betablockers	64 (60%)
ASA	78 (73%)
Long acting nitrates	10 (9%)

4.3 Methods

4.3.1. Imaging Protocols

4.3.1.1 CT Imaging

All CT and PET scans in studies I, III, IV and V were performed by using a hybrid 64-row PET/CT scanner (GE Discovery VCT, General Electric, Wisconsin, USA). After initial lateral and frontal scout images, a preliminary non-enhanced data set was acquired to calculate the calcium score and to optimize the field of view for the CTA. 16 x 2.5 mm collimation, 120 kV tube voltage and 200 mAs tube current were used. The data in the contrast enhanced studies, both in sequential and spiral modes, were collected by using the following parameters: 64 x 0.625 mm collimation, gantry rotation time of 350 msec, tube voltage of 100-120 kV and 600-750 mAs tube current both depending on patient size. In the sequential mode, the pitch was always 1.0 with 5 mm overlap between the slice stacks. Prospective ECG triggering determined the centre of the acquisition (end diastole, 75% of the cycle) while the width of this window was set between 100 and 200 ms according to HR.

In spiral mode, the pitch was set between 0.16 and 0.24 according to HR. Routinely used ECG modulation software reduced radiation outside the 40-80% phase window by a maximum of 40%.

Study II was a multi-center study performed at 5 European sites. MDCT coronary angiography was performed with 2 different 16-slice MDCT scanners (Aquilion 16, Toshiba Medical Systems, Japan n=39, and Discovery STE, General Electrics, USA, n=8) and 3 different 64-slice MDCT scanners (Aquilion 64, Toshiba Medical Systems, Japan, n=202, LightSpeed VCT, General Electrics, USA, n=19, and Discovery VCT, General Electrics, USA, n=30). In the absence of contraindications, patients with heart rate ≥65 beats/min were administered beta-blockers (50-100mg oral or 5-10mg intravenous metoprolol). First, a prospective coronary calcium scan without contrast agent was performed, followed by 16- or 64-slice CTA.

The total radiation dose of the studies was recorded and the effective dose of the CT calculated with a method proposed by the European Working Group for Guidelines on Quality Criteria in CT (EC99 1999). The effective dose is derived from the product of the DLP and a conversion coefficient for the chest as the investigated anatomic region. This conversion coefficient ($k=0.017\ mSv \cdot mGy^{-1} \cdot cm^{-1}$) is averaged between male and female models.

4.3.1.2 PET imaging (Studies I, III-V)

Rest-stress perfusion PET was performed immediately after CTA. ^{15}O-labeled water (900-1100 MBq) was injected (Radiowater Generator, Hidex Oy, Turku, Finland) at rest as an intravenous bolus over 15s at an infusion rate of 10 ml/min. Dynamic acquisition of 4 min 40 s was performed (14 x 5 s, 3 x 10 s, 3 x 20 s and 4 x 30 s). After a 10 min delay following the first injection, a stress scan was performed during adenosine-induced hyperaemia. Adenosine was started 2 minutes before the scan start and infused to the end of the scan at 140 µg/kg body weight/min.

4.3.1.3 Invasive Angiography and FFR (Studies III-V)

All ICAs were performed on a Siemens Axiom Artis coronary angiography system (Siemens, Munich, Germany). In the presence of intermediate stenoses, FFR measurement was performed using ComboMap® pressure/flow instrument and a 0.014-inch BrightWire® pressure guide wires (Volcano Corp., Rancho Cordova, CA, USA). The pressure was measured distally to the lesion during maximal hyperaemia induced by 18 µg intra-coronary boluses of adenosine with simultaneous measurement of aortic pressure through the coronary catheter. FFR was calculated as the ratio between mean distal pressure and mean aortic pressure.

Quantitative analysis of coronary angiograms (QCA) was performed by using software with automated edge detection system (Quantcore, Siemens, Munich, Germany) by an experienced reader blinded to the results of PET, CTA and FFR. 17 standard segments were analyzed.

The combined PET/CT protocol used in studies I and III-V is demonstrated in **Figure 2**.

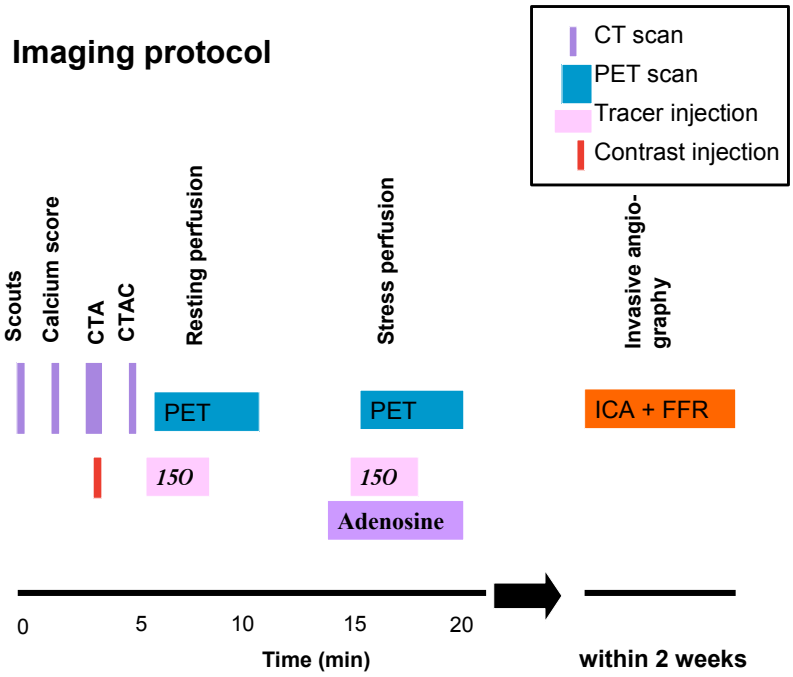

Figure 2. The combined PET/CT protocol used in studies I and III-V

4.3.2 Data Analysis

4.3.2.1 Study II

The CT data analysis was performed in each center by two experienced observers who had no knowledge of the patient's medical history and symptom status; disagreement was solved by consensus or evaluation by a third observer. Standardized MDCT data evaluation methodology and scoring system were used in each center.

4.3.2.2 Studies I, III-V

All data were sent to a GE ADW 4.4 workstation for analysis. For CT analysis, all phases (0-90% in 10% intervals and the 75% phase) of the retrospectively gated spiral data sets were reconstructed while all available data (usually 65-85% phases) of the sequential sets were reconstructed in 5% intervals. The analysis was performed both on per patient and per main vessel. In CTA, the stenoses ≥50% were classified as significant. Image quality and reader confidence were

assessed in a scale of 1 to 5. In study I, a single blinded reader analyzed the images 3 times. In studies IV-V, the images were analyzed by two experienced readers in concensus.

PET Images (Studies III-V) were quantitatively analyzed with Carimas™ software by an experienced reader blinded to other results and clinical data. Both standard polar plots and parametric volume of the heart were produced, allowing image fusion with CTA using ADW 4.4 software (CardiIQFusion). In study III, 20 randomly selected ^{15}O-labeled water PET scans from 10 patients (one rest scan and one stress scan from each patient) were analyzed by four observers. The observers, though educated as medical doctors, differed in experience. Before the actual analysis the observers were given the identical training. All the observers were blinded to a subject's characteristics, clinical data, and scan type (rest or stress) as well as the results of the other readers. Each observer performed the analysis of each subject twice in separate sessions 1-2 weeks apart so producing two *repeats* of each subject. The observers analysed the images through standardized consecutive steps: reoriented the images, defined the heart axes, identifying the base and the apex of the heart, accepted or modified automatically generated regions of interests (ROIs), and finally calculated and reported the results. The obtained results represented global MP, perfusion in different coronary artery territories and the segmental MP. The accuracy of perfusion imaging was then applied in clinical situation in 48 consecutive symptomatic patients with suspected CAD who were referred for ICA. In ICA 50% (or more) luminal narrowing was considered significant. The cut-off value of absolute perfusion analysis for the optimal detection of coronary stenoses was first assessed and thereafter the accuracy was calculated. The PET perfusion analysis workflow of Studies III-V is presented in **Figure 3.**

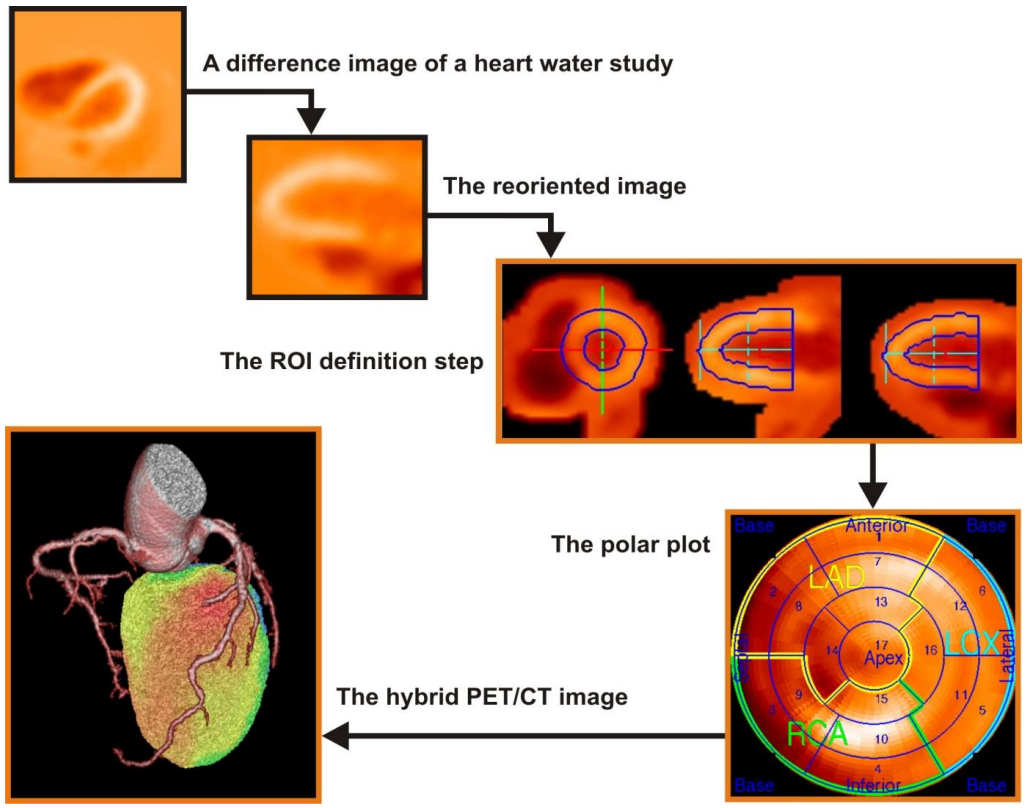

Figure 3. The PET perfusion analysis workflow of Studies III-V

In PET, quantitative values during stress were classified as validated earlier: absolute myocardial stress perfusion of less than 2.5 mL/g/min was considered abnormally low. In addition, a receiver operating characteristic (ROC) curve was calculated to determine optimal cut-off points of MBF stress alone and the MBF from the regions with stenosed vessel in CTA (studies IV-V).

CT and PET images were fused to assign the stenoses to the areas of MP (studies IV-V). The results were interpreted as follows: 1) When both CTA and perfusion were normal, the vessel was normal, 2) when CTA detected ≥50% stenosis that was assigned to abnormal perfusion, the vessel was significantly stenosed, 3) when CTA detected ≥50% stenosis that was assigned to normal perfusion, the vessel was regarded as non-significantly stenosed 4) When CTA detected no significant stenosis but a vessel was assigned to abnormal perfusion, the vessel was graded as non-significantly stenosed and was suggested to be a sign of micro-vascular disease. In ICA, luminal diameter narrowing ≥50% was considered significant. When FFR was available, stenoses with FFR >0.8 were classified as non-significant, regardless of the degree of narrowing.

4.3.3 Statistical Methods

4.3.3.1 Study II

Multivariable logistic regression analyses (backward stepwise with retention level set at 0.1) were used to evaluate the relationship between demographic and clinical data (age, gender, coronary risk factors, symptoms, pre-test likelihood of CAD and history of AF) and the presence of CAD and obstructive CAD at CTA. The diagnostic accuracy of CTA for the detection of obstructive (≥50% luminal narrowing) coronary artery stenoses was assessed in the subgroup of patients who underwent ICA. The sensitivity and specificity, including 95% confidence intervals (CI), were calculated by using ICA as the reference standard. A p value <0.05 was considered statistically significant. Statistical analyses were performed with SPSS software (version 14.0, SPSS Inc, Chicago, Ill, USA).

4.3.3.2 Study III

We used an intra-class correlation coefficient (ICC) for the assessment of reliability of repeated quantitative measurements. ICC measures consistency or conformity between two or more quantitative measurements. The basic idea of ICC is to compare the variability due to repeated measurements from the same object to the total variation which is induced by all measurements and all the objects. Here, the ICC informed on intra-observer correlations between the repeats, and was used to determine the intra-observer reproducibility of the analysis as such with no division into "rest" and "stress" subjects. The ICC values were interpreted as follows: intraclass correlation coefficient values of 0.00 to 0.20 represented *slight* agreement, 0.21 to 0.40 *fair* agreement, 0.41 to 0.60 *moderate* agreement, 0.61 to 0.80 r *substantial* agreement, and > 0.81 *very good* agreement.

The intra-observer and inter-observer differences were calculated based on the linear mixed model. These differences treated the "rest" and the "stress" subjects separately. Should the compared values be equal to each other, the differences between them would equal zero. However, in practice, it is enough to be sure that the 95% confidence interval of the difference includes zero, meaning the difference between them is not significant. The obtained difference values were expressed in standard MP units.

4.3.3.3 Studies IV-V

Sensitivity, specificity, PPV, NPV and accuracy were calculated for each imaging method (PET, CT, and PET/CT). A ROC analysis curve was performed for both relative and absolute assessment of MBF to reconfirm the best cut-off points during stress in the study population. McNemar`s test was performed to compare accuracy of PET, CT and PET/CT against the reference method (i.e., ICA with FFR). A p-value < 0.05 was considered statistically significant. The statistical tests were performed with SAS version 9.1.

5. RESULTS

5.1. Radiation Dose and Feasibility of Sequential Coronary CTA and PET/CT (Study I)

No significant differences were present between the two patient populations (sequential vs. spiral imaging) in terms of patient size (body mass index, BMI) or HR (64.5±14.1 vs. 56.6±5.9 BPM, p=0.13) during the acquisition.

There were no significant differences between the sequential and spiral groups in terms of either image quality or reader confidence. Mean image quality was 3.6/5 in the spiral group and 3.7/5 in the sequential group while the subjective diagnostic confidence of the reader was 4.0/5 and 4.3/5 in the same two groups, respectively. The mean effective radiation dose was 19.3±3.6 mSv in the spiral group (range, 15.0 – 26.0 mSv) and 7.6±0.8 mSv (range, 6.0 – 8.4 mSv) in the sequential group. The mean dose reduction was 60.4% when using sequential method. This reduction was statistically significant ($p<0.001$).

In the second part, the sequential technique was feasible in 53 of 61 patients (87%). The remaining eight patients (13%) had heart rates either too high (>65 BPM) or unstable even after maximum dose of i.v. metoprolol, or medication could not be given due to contraindications. These patients were studied with the spiral mode. Image quality between the spiral and sequential groups were not compared in this part of the study because of obvious pre-selection bias. All studies, however, were of diagnostic quality.

The main results of the assessments of image quality, reader confidence and radiation dose of the patients of the first part of study I are presented in **Table 3**.

Table 3. Assessment of image quality, reader confidence and radiation dose

PT #	GENDER	PROTOCOL: 1=SPIR, 2=SEQ	BMI	HR PRIOR TO ACQUISITION	MG METOPROLOL	NITRATE (Y/N)	HR DURING ACQUISITION	OVERALL IMAGE QUALITY 1-5 (1=POOR,5=EXCELLEN)	DG CONFIDENCE 1-5 (1=POOR 5=EXCELLENT)	DLP (mGy*cm)	CALC.EFF.DOSE (MsV)
1	F	1	20.4	63	25	Y	61	4	5	866	14.7
2	F	1	22.4	80	25	Y	55	5	5	1064	18.1
3	F	1	25.7	65	10	Y	50	5	5	1076	18.3
4	F	1	28.3	64	10	Y	67	3	4	1074	18.3
5	M	1	32.1	58	5	Y	63	3	4	1369	23.3
6	F	1	43.0	75	20	Y	98	1	2	1538	26.1
7	F	1	24.5	86	30	Y	77	3	3	1053	17.9
8	F	1	20.4	59	5	Y	55	5	5	1005	17.1
9	F	1	28.7	64	15	Y	55	3	3	1364	23.2
10	M	1	23.7	78	25	Y	64	4	4	961	16.3
Mean±SD			**26.9±6.8**	**69.2±9.7**	**17±9.2**		**64.5±14.1**	**3.6±1.3**	**4.0±1.1**	**1137±213**	**19.3±3.6**
11	*M*	*2*	*27.6*	*68*	*15*	*N*	*61*	*4*	*4*	*470*	*8.0*
12	*F*	*2*	*20.9*	*75*	*25*	*Y*	*61*	*4*	*5*	*437*	*7.4*
13	*F*	*2*	*32.0*	*68*	*20*	*Y*	*61*	*3*	*4*	*371*	*6.3*
14	*F*	*2*	*39.2*	*50*	*0*	*N*	*62*	*3*	*4*	*495*	*8.4*
15	*M*	*2*	*26.9*	*50*	*0*	*Y*	*51*	*4*	*4*	*494*	*8.4*
16	*M*	*2*	*30.1*	*52*	*0*	*Y*	*52*	*4*	*5*	*465*	*7.9*
17	*M*	*2*	*24.8*	*48*	*0*	*Y*	*44*	*5*	*5*	*491*	*8.3*
18	*F*	*2*	*24.1*	*64*	*15*	*Y*	*60*	*5*	*5*	*436*	*7.4*
19	*M*	*2*	*30.3*	*74*	*15*	*Y*	*56*	*2*	*3*	*472*	*8.0*
20	*M*	*2*	*31.1*	*73*	*30*	*Y*	*58*	*3*	*4*	*366*	*6.2*
Mean±SD			**28.7±5.1**	**62.2±11.0**	**12.0±11.4**		**56.6±5.9**	**3.7±0.9**	**4.3±0.7**	**450±48**	**7.6±0.8**

In the second part, all patients underwent hybrid PET/CT imaging, of which the radiation doses are shown in **table 4**

Table 4. Radiation dose (mSv) of spiral and sequential hybrid PET/CT

Scan Type	**CTA + calcium score**	**^{15}O-water PET**	**combined protocol**
Spiral (n=8)	19.9 ± 3.2	2.1 ± 0.1	22.0 ± 3.2
Sequential (n=50)	7.6 ± 1.1	2.0 ± 0.2	9.5 ± 1.5
N=58	*p<0.001*	*p<N.S*	*p<0.001*

The mean total radiation dose of a sequential CT (calcium score and contrast enhanced CTA) was 7.6±1.1 mSv (range, 5.9 – 10.2 mSv) whereas it was 19.9±3.2 mSv when using the spiral protocol. The mean radiation dose of the dual (rest-stress) ^{15}O-water PET perfusion studies was 2.1±0.1 mSv in the spiral patients yielding a total dose of 22.0±3.2 mSv. Because the PET protocol remained unchanged regardless of the CT mode, the dose in PET was almost similar to the

spiral group (mean, 2.0±0.2 mSv). The mean total dose of the combined study was 9.5±1.5 mSv with sequential CT acquisition. This analysis included 50 patients because PET failed in three subjects due to a technical failure in the ^{15}O-water system.

5.2. Prevalence of CAD in Patients with Atrial Fibrillation (Study II)

5.2.1. Patient Characteristics

AF and non-AF groups did not differ as to mean age (61±11 vs. 59±10 years), male gender (67% vs. 65%), symptomatic status and pre-test likelihood of CAD. A history of typical or atypical angina pectoris was present in 42% of AF patients and in 43% of non-AF patients and the pretest likelihood of CAD according to Diamond and Forrester was low, intermediate, and high, respectively, in 59%, 25% and 16% of the AF patients and in 58%, 28% and 14% of non-AF patients. AF patients, as compared to non-AF patients, were less frequently diabetics (13% vs. 28%, p <0.001) and smokers (21% vs. 31%, p=0.027). Overall, the prevalence of ≥ 3 coronary risk factors was not statistically different between the two groups.

5.2.2. Coronary Artery Calcium Score

Coronary artery calcium score was successfully performed in 133 (89%) AF patients and in all non-AF patients. The median Agatston calcium score did not differ between AF patients and non-AF patients (27, interquartile range 0-308, vs. 75, interquartile range 0-350; p=0.19). The prevalence of no calcium and minimal, mild, moderate and severe coronary calcifications was not statistically different between the two groups, although coronary arteries with no calcium was less frequently observed among AF patients.

5.2.3. CTA

CTA was successfully performed in all the patients of the study population. Mean heart rate during the CT scan was 64±6 beats/min among AF patients and 65±9 beats/min among non-AF patients (p=0.24). 28 (18%) AF patients were classified as having no CAD based on CT, whereas 61 (41%) showed non-obstructive CAD and at least one significant (≥ 50%) luminal narrowing was observed in the remaining 61 (41%) patients. The prevalence of CAD among non-AF patients was significantly lower: 47 (32%) were classified as having no CAD, while 61 (41%) showed non-obstructive CAD and 40 (27%) had obstructive CAD, based on CT (p=0.010 compared to AF patients). Obstructive single-vessel disease was present in 35 (23%) AF patients, whereas obstructive left main (LM) and/or proximal left anterior descending (LAD) disease was present in 37 (25%) AF patients. Multi-vessel disease was observed in 26 (17%). Non-AF patients showed a significantly

lower prevalence of obstructive single-vessel disease and obstructive LM and/or proximal LAD disease, as compared to AF patients, but not a significantly lower prevalence of multi-vessel disease. Obstructive single-vessel disease was observed in 19 (13%) non-AF patients, obstructive CAD in the LM and/or proximal LAD in 15 (10%) and multi-vessel disease in 21 (14%) (p=0.024, p=0.001 and p=0.53, respectively, compared to AF patients). Due to motion artifacts, 39 (1.5%) segments in the AF group and 38 (1.5%) segments in the non-AF group were excluded from the segment-based analysis, respectively. A significantly higher number of diseased coronary segments was present in the AF group, as compared to non-AF group (5.5±3.9 vs. 4.0±4.0, p=0.001; 1.1±1.9 vs. 0.8±1.7, p=0.010 and 4.4±3.2 vs. 3.2±3.3, p=0.001, respectively).

5.2.4. Diagnostic Accuracy of CTA

79 patients underwent ICA. The overall number of obstructive (≥50% luminal narrowing) coronary artery stenoses was 151. The sensitivity and specificity of CTA was 92.1% (95% CI 86.5%-95.8%) and 96.4% (95% CI 95%-97.4%), respectively.

The results of Study II are summarized in **Figures 4-6:**

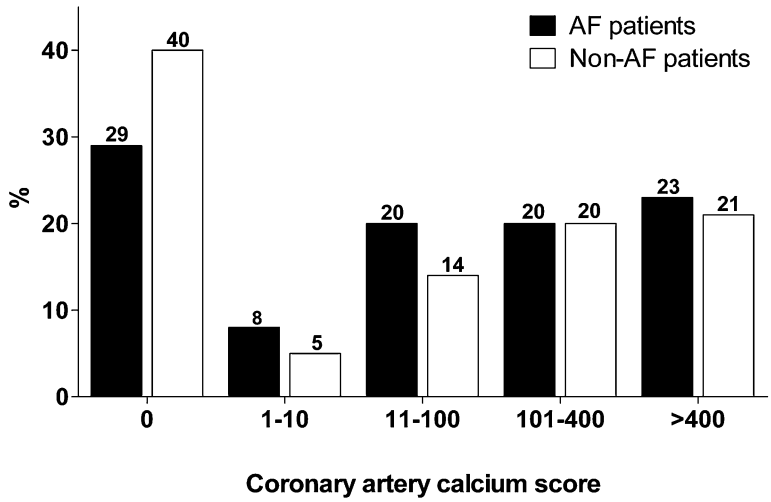

Figure 4. Bar graph demonstrating the coronary artery calcium score categories in patients with and without history of paroxysmal or persistent AF. Solid bars: AF patients; open bars: non-AF patients. P=0.31 for comparison between the two groups.

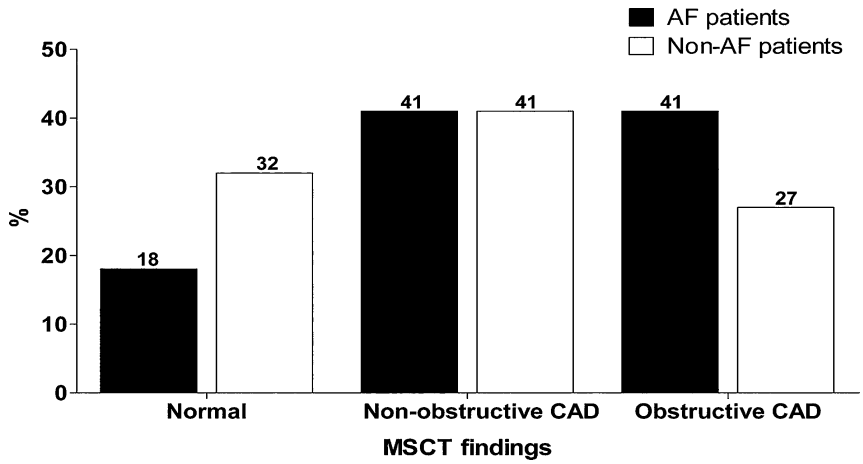

Figure 5. Prevalence of CAD in patients without and with history of paroxysmal or persistent atrial fibrillation (AF). Solid bars: AF patients; open bars: non-AF patients. *P*=0.010 for comparison between the two groups.

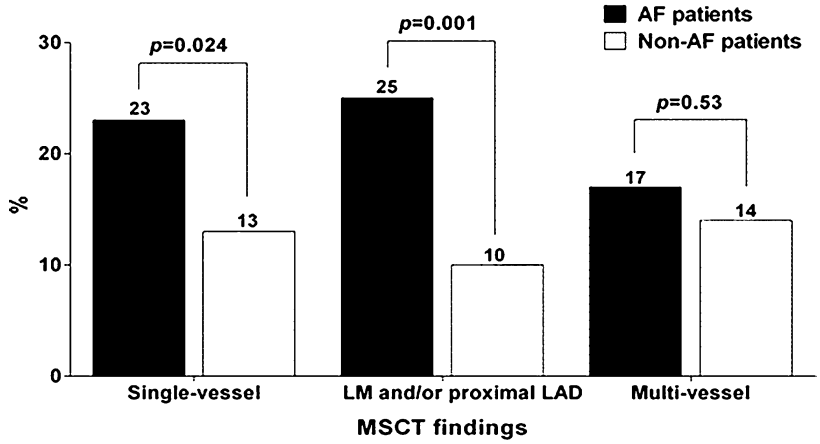

Figure 6. Prevalence of obstructive single-vessel, LM, or proximal LAD CAD and of multivessel disease in patients with and without history of paroxysmal or persistent AF. Solid bars indicate patients with AF; open bars patients without AF.

5.3. Quantification of Myocardial Perfusion with ^{15}O-water PET: Accuracy and Reproducibility of a Novel Software (Carimas™) (Study III)

In **Figure 7** (the O_I observer) all the segmental MPs were plotted separately for "rest" and "stress" (two measurements of the segment 3 are missing, basal inferoseptal wall) (the *r* values were 0.974 and 0.978, and the repeatability coefficients – 0.145

ml/g/min and 0.389 ml/g/min at rest and under stress, correspondingly). The MP values in segments belonging to the three coronary artery territories are plotted in **Figure 8**. **Figures 9-12** summarize further intra- and interobserver differences.

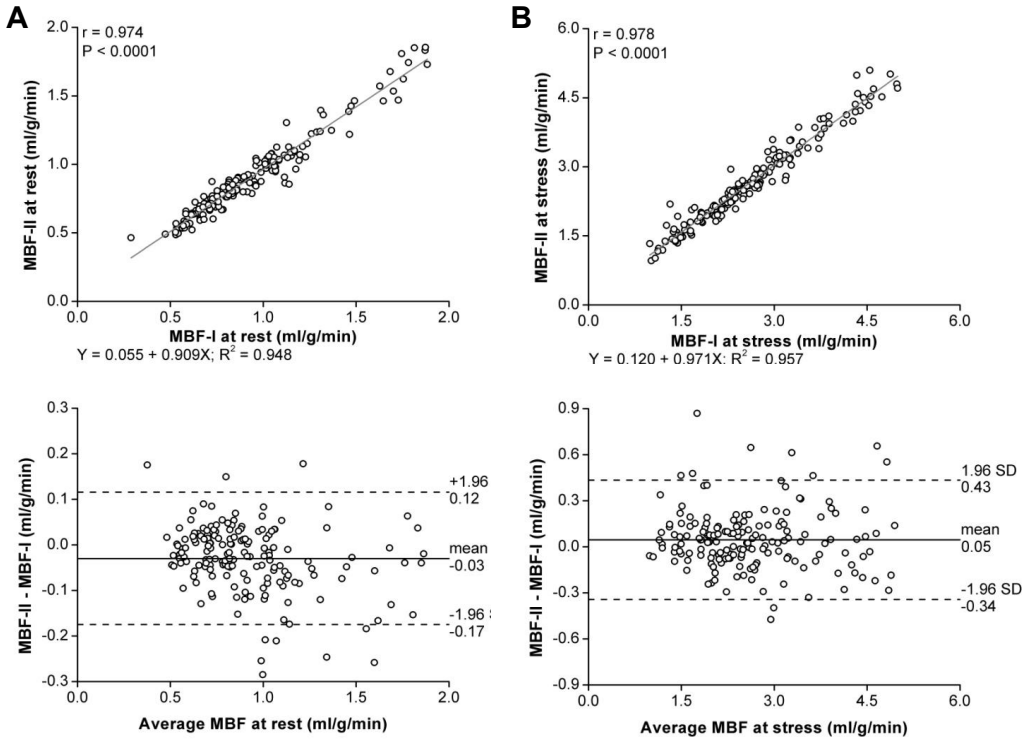

Figure 7. Reproducibility of MBF in the first observer (O_I) at rest in 168 ROIs of 10 subjects (A) and at stress in 170 ROIs of 10 subjects (B). (Top) Regression lines are drawn. (Bottom) Bland-Altman plots.

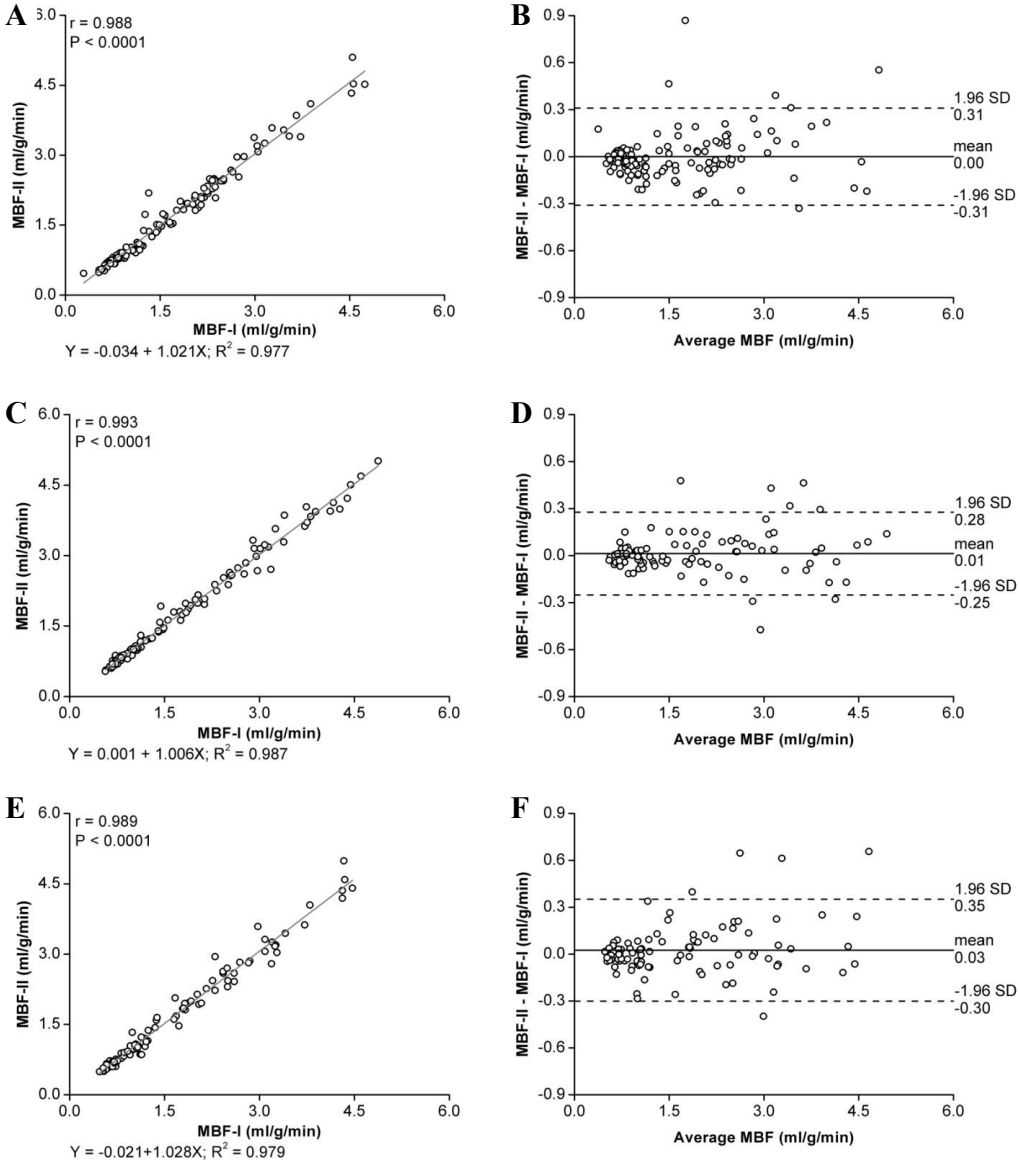

Figure 8. Linear regression analysis and Bland-Altman plots comparing MBF measurement replicates in the observer O_I by coronary artery territories: LADwa (A and B), LCX (C and D), and RCA (E and F).

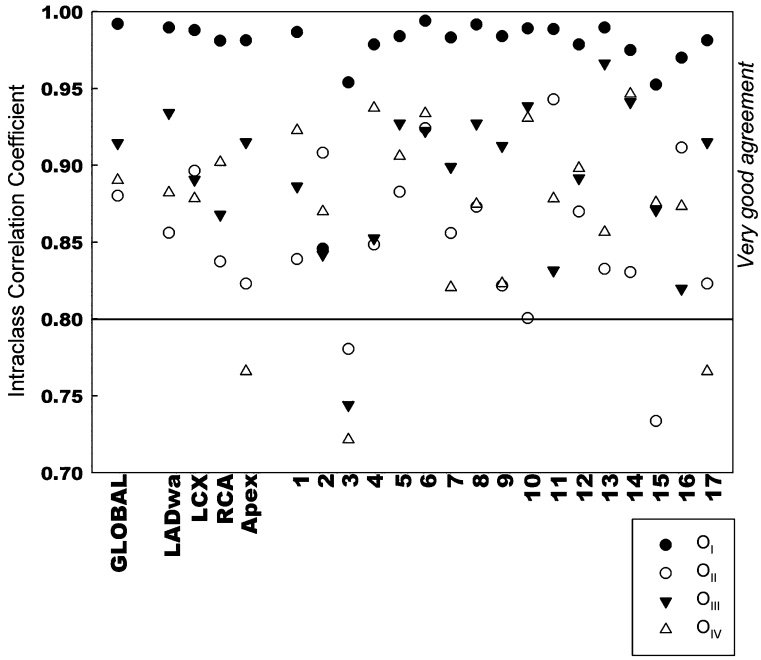

Figure 9. Intraclass correlation coefficient (ICC) for intraobserver reproducibility. The ICC values above 0.80 (the horizontal line) indicate very good agreement and values from 0.61 to 0.80 represent substantial agreement.

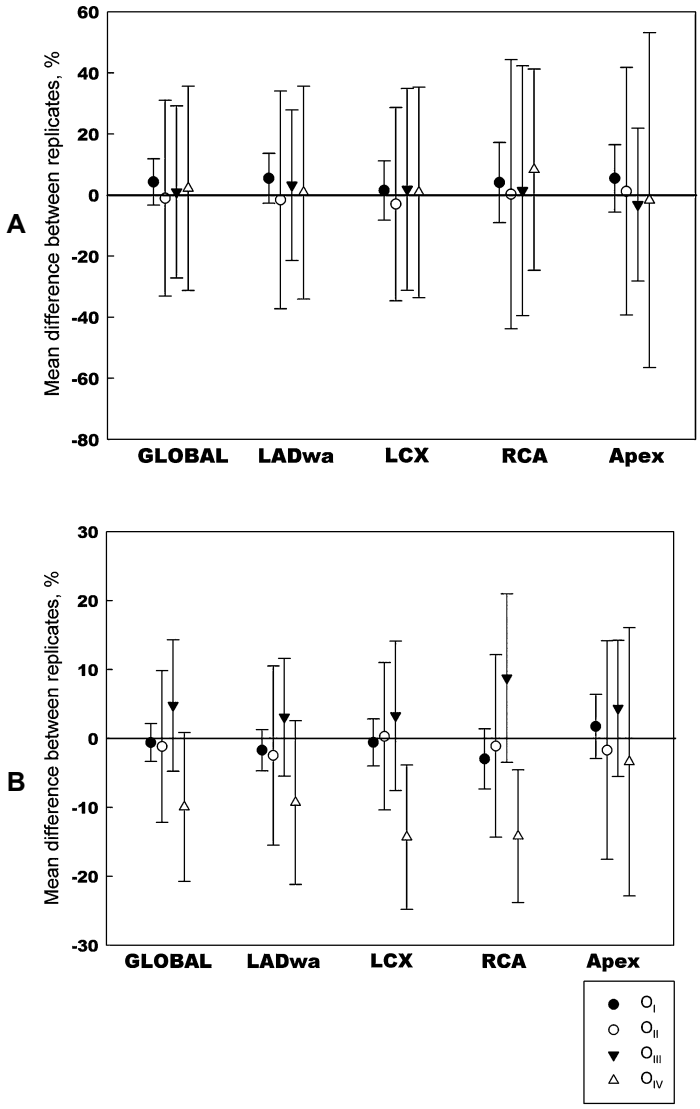

Figure 10. Mean differences (and 95% confidence intervals) between replicates in the observers at rest (A) and under stress (B). The difference is not significant if its confidence interval crosses the zero line.

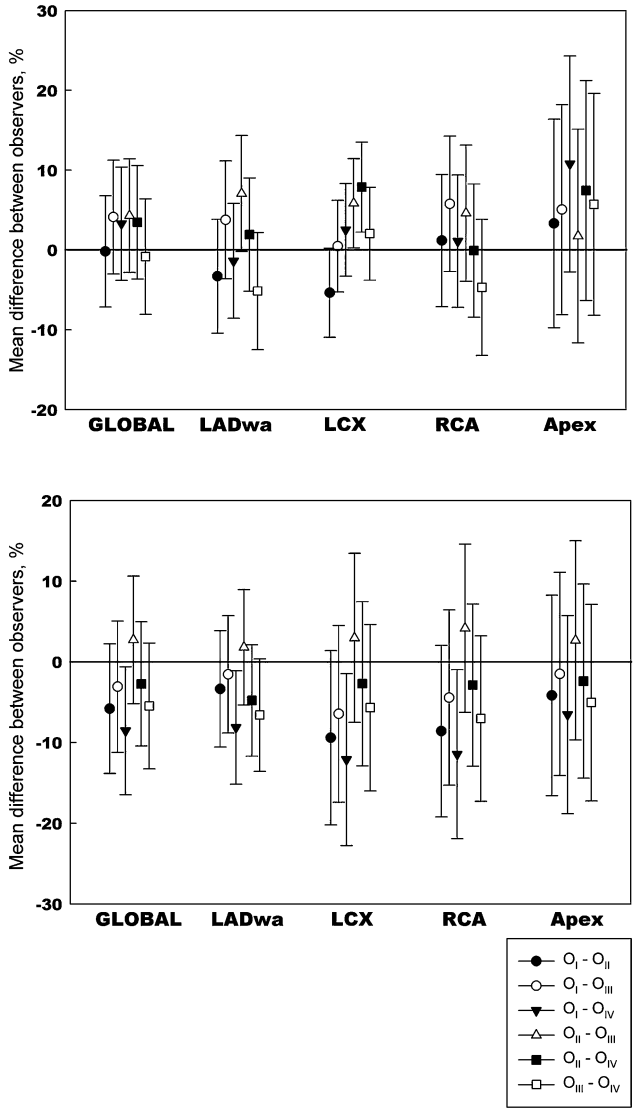

Figure 11. Mean differences (and 95% confidence intervals) between the observers at rest (A) and under stress (B). The difference is not significant if its confidence interval crosses the zero line.

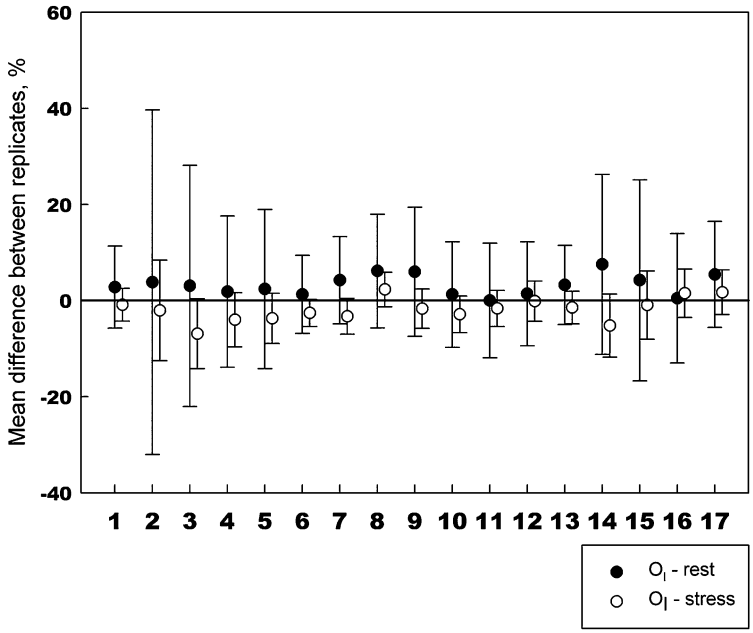

Figure 12. Segmental mean differences (and 95% confidence intervals) between the replicates in the first observer (O_I) at rest and under stress.

5.3.1. Analysis of Global Perfusion

Reproducibility was very good for the global perfusion. The most experienced observer (O_I) had the highest ICC (0.99) while O_{II} had the lowest (0.88). In O_{III} and O_{IV} the ICC was 0.91 and 0.89 correspondingly. The intra-observer reproducibility was good as well: the 95% confidence intervals of the differences between repeats included zero both at rest and during stress indicating that the differences were not significant. This indicated that repeated analysis by the same observer produced nearly same results. The absolute values of difference were close to zero: at rest the highest value was 4.3% in O_I, and at stress it was somewhat higher in the novice O_{IV} (9.9%). The inter-observer reproducibility was also good except for the difference between the most experienced (O_I) and the novice (O_{IV}) observers at stress.

5.3.2. Analysis of Perfusion in the Coronary Artery Territories

The highest ICC values were observed in the most experienced observer (O_I): in the three territories it was above 0.98. The lowest values were found in O_{II}: 0.86 in LADwa, 0.84 in RCA, and in O_{IV} – 0.88 in LCx, all these values still falling into the category of the *very good* agreement. The intra-observer reproducibility was good except in the novice observer (O_{IV}) at stress in LCx and RCA: the absolute values of difference were 14.3% and 14.2% correspondingly. As to the inter-observer

reproducibility, the systematic difference was again found between the most and the least experienced observers O_I and O_{IV} at stress.

5.3.3. Segmental Perfusion

The vast majority of segmental ICC values and all the values in the most experienced observer (O_I) were above 0.81 indicating very good agreement for segmental results. The lowest segmental ICC values were observed in the basal inferoseptal segment (3rd). In O_{IV} the ICC for this segment was 0.72, in O_{III} – 0.74 and in O_{II} – 0.78; however, in the most experienced observer (O_I) it was still excellent (0.95). The lowest ICC in this experienced observer was 0.84 in the basal anteroseptal segment (No. 2); all the other ICCs in O_I were above 0.95.

The intra-observer differences in segmental values were also analyzed with no significant differences found in the most experienced observer or in observer OII. However, in the other two observers significant differences were found between the repeats at stress. In observer OIII it was 12.0% in the 15th segment while there were significant differences present in OIV in several segments, with the largest one being 15.4% in segment 10. A significant inter-observer difference was found at rest between observer OI and observer OII in basal segments 1, 5 and 6, and in the 12th segment. The maximal difference was 10.2% in the 6th segment. The results of the observer OII were significantly different from all the other observers as well. At stress, differences were found between OI and OII in segments 1 and 11 (11.7%, 12.9% correspondingly) and between OI and OIV in segments 1 and 14 (11.9%, 12.1%).

5.3.4. Clinical Accuracy of the Analyses

The incidence of CAD in the clinical population was 50% in ICA. All 48 patients (37 males and 11 females) were successfully analyzed. When compared against existence of stenosis of 50% or more, the absolute MBF of <2.5 ml/g/min was found to be the best cut-off point in identifying significant coronary stenosis. With this cut-off point, the positive and negative predictive values and accuracy of MP results in detecting significant CAD were 91%, 88% and 90%, respectively.

5.4. Detection of Significant Coronary Artery Disease with Cardiac PET/CT (Study IV)

5.4.1. General

44 patients out of 107 (41%) had stenoses ≥50% in their coronary arteries in ICA. Significant lesions after invasive angiography and FFR were detected in 40 patients. In 18 of them, the lesions were either total occlusions or extremely tight (>90%) stenoses in which FFR was not possible. Four other patients had intermediate (30%

to 70%) stenoses in which FFR could not be performed because of scheduling or technical reasons. In patients without FFR, quantitative coronary angiography ≥50% was considered positive and the vessel was graded accordingly. Overall, 80 of 428 arteries were significantly stenosed by the combination of ICA and FFR. Lesions after invasive angiography and FFR were detected in 40 patients. In 18 of them, the lesions were either total occlusions or extremely tight (>90%) stenoses in which FFR was not possible. There were 4 other patients with intermediate (30-70%) stenoses in which FFR could not be performed due to scheduling or technical reasons. In patients without FFR, QCA >50% was considered positive and the vessel graded accordingly.

5.4.2 CT Angiography

CTA alone had PPV of 81%, NPV of 97% and accuracy of 90% per patient while the corresponding figures of the vessel analysis were 76%, 94% and 91%. In most discrepant cases, CT overestimated the degree of stenosis. There were only 2 patients in whom CAD was missed but in 10 additional ones at least one significantly stenosed vessel was not detected. These lesions were evenly distributed into different coronary branches.

5.4.3 PET Perfusion Imaging

Perfusion at rest was normal in all patients. The stress PET perfusion in patient based analysis had a PPV, NPV and accuracy of 86%, 97% and 92%, respectively. The corresponding values for vessel analysis were 78%, 98% and 92%. 2 patients had false negative PET perfusion results with ≥50% stenosis detected at ICA but FFR could not be performed in these patients. 6 patients had false positive PET perfusion, of which 5 had diffusely reduced myocardial perfusion but no corresponding epicardial coronary disease; in one patient a regional perfusion defect was incorrectly diagnosed. In vessel analysis, 4 other patients exhibited at least one perfusion abnormality in a region without significant epicardial disease.

5.4.4 Hybrid Imaging

Most patients with false positive CTA had normal PET perfusion, thus correcting the diagnoses (see criteria above). On the other hand, 4 out of 5 patients with false positive PET findings had diffuse perfusion abnormalities but no epicardial disease in CTA, the cases correctly identified in hybrid imaging. In one case, there was diffusely reduced perfusion with one stenosed vessel. In addition, CTA vessel analysis helped to assign the perfusion zones of the LCx and the right coronary artery (RCA) because the dominant vessel is easily distinguished. In combined analysis only 2 false negatives and no false positives were diagnosed. PPV, NPV and accuracy were 100%, 98% and 98%, correspondingly.

In the vessel analysis the PPV, NPV and accuracy of hybrid imaging were 96%, 99% and 98%, correspondingly. In 4 vessels with intermediate (30-70%) stenoses in CTA, hybrid imaging was abnormal but invasive tests supported non-significant lesions. In 3 other vessels, hybrid imaging suggested non-significant lesions but ICA showed >50% stenosis. In all of these vessels, however, FFR was not performed successfully but the vessels were classified according to ICA alone. Hybrid imaging was more accurate per patient than CTA (p=0.0039) or PET alone (p=0.014). It was also better in the vessel based analysis (p<0.0001 and p<0.0001, correspondingly).

The results are summarized in **Tables 5-6** (hybrid modality) and **Figure 13**. **Table 7** exhibits the characteristics of the 5 patients with suspected micro-vascular disease (i.e., those with diffusely reduced perfusion without accompanying epicardial lesions). **Table 8** summarizes the discrepant findings between hybrid imaging and the reference method, ICA and FFR.

Table 5. Results per patient

N=104	**ICA + FFR**		
		+	-
CTA-PET hybrid	**+**	36	0
	-	2	66

Table 6. Results per vessel

N=416	**ICA + FFR**		
		+	-
CTA-PET hybrid	**+**	71	3
	-	5	337

Figure 13a: Patient Analysis against ICA+FFR

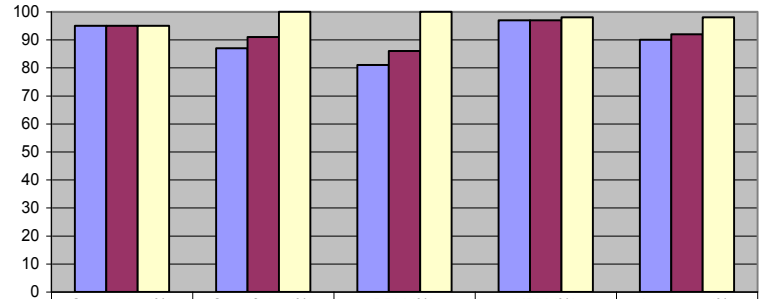

	Sensitivity (%)	Specificity (%)	PPV (%)	NPV (%)	Accuracy (%)
MDCT	95	87	81	97	90
PET	95	91	86	97	92
MDCT-PET hybrid	95	100	100	98	98

Figure 13b: Vessel Analysis against ICA+FFR

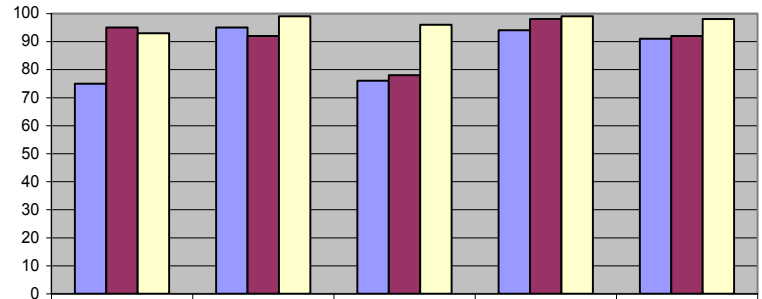

	Sensitivity (%)	Specificity (%)	PPV (%)	NPV (%)	Accuracy (%)
MDCT	75	95	76	94	91
PET	95	92	78	98	92
MDCT-PET hybrid	93	99	96	99	98

Figure 13: Sensitivity, specificity, positive and negative predictive values and accuracy of stand-alone CT, PET and hybrid imaging against combined ICA and FFR. **13a:** Analysis per patient. Hybrid imaging was statistically more accurate than either CTA alone ($p=0.0039$) or PET alone ($p=0.014$). The difference between CTA and PET was not significant ($p=0.32$): **13b:** Analysis per vessel. Hybrid imaging was statistically more accurate than either CTA alone ($p<0.0001$) or PET alone ($p<0.0001$). The difference between CTA and PET was not statistically significant ($p=0.08$).

Table 7. Patients with diffuse perfusion abnormalities but non-stenotic epicardial coronary arteries

Patient	gender	smoker	Body Mass Index	Diabetes	Family history of CAD	PET stress MBF (ml/g/min)	Agatston score
P006	male	no	21.8	no	no	**1.7-2.1**	117
P010	male	yes	33.1	no	yes	**1.2-2.3**	6
P077	male	no	19.4	no	yes	**1,4.1,8**	16
P079	female	no	19.1	no	yes	**1.6-2.0**	0
P090	male	yes	25.7	no	yes	**1.7-1.8**	0

Table 8. Discrepant findings between PET/CT and ICA + FFR

Patient	Vessel	CTA stenosis	PET stress MBF (ml/g/min)	Invasive stenosis (QCA)	Suspected explanation for discrepancy
P020	LAD	50-69%	3.1 (normal)	55%	Mid LAD intermediate stenosis, no successful FFR
P020	RCA	50-69%	2.1 (abnormal)	39%	Two stenoses distally in RCA, no FFR.
P031	RCA	50-69%	2.0 (abnormal)	40%	Severe calcifications in CTA and reduced flow, in ICA intermediate stenosis in mid RCA, no FFR
P033	LAD	>70%	3.0 (normal)	50-60%	Proximal and mid LAD intermediate stenoses, no successful FFR
P070	LAD	50-69%	3.1 (normal)	50%	50% stenosis was interpreted as significant, no FFR.
P071	LM	<30%	2-2.3 (abnormal)	50%	Severe triple vessel disease with global reduction in perfusion, CTA did not note LM stenosis
P084	RCA	50-69%	1.9 (abnormal)	39%	Distal RCA intermediate stenosis, no FFR
P094	LAD	30-49%	3.2 (normal)	61%	No FFR of LAD

Figures 14-15 present ROC tables showing that MBF value of 2.5 ml/g/min gives the best combination of sensitivity and specificity both with and without CTA information. If the cut-off value was reduced the specificity was slightly improved at the cost of sensitivity. The estimated probability of CAD based on ROC analysis demonstrated that practically all regions with MBF below 2.0 ml/g/min were abnormal

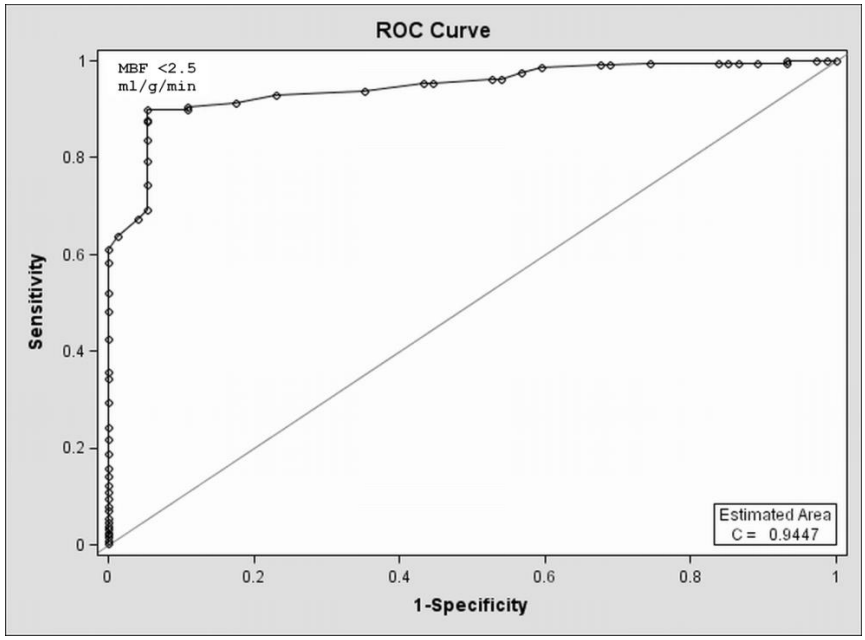

Panel a

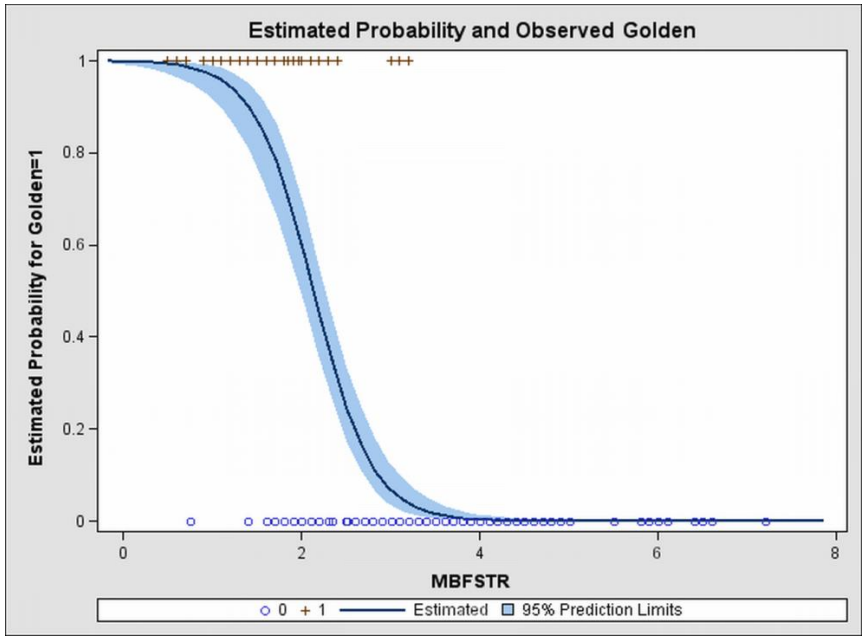

Panel b

Figure 14: A receiver operating characteristic (ROC) analysis. **Panel a**: ROC curve of vessel-based PET perfusion against gold standard with cut-off values. **Panel b**: Estimated probability of significant CAD against stress MBF. MBFSTR=stress MBF; Golden= Combined analysis of ICA and FFR.

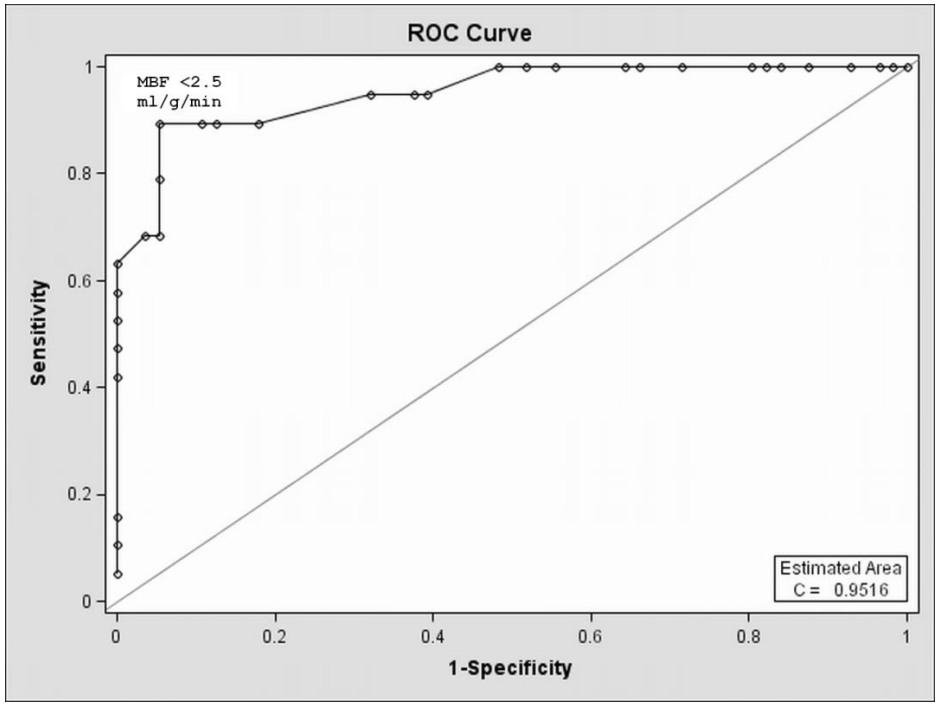

Panel c

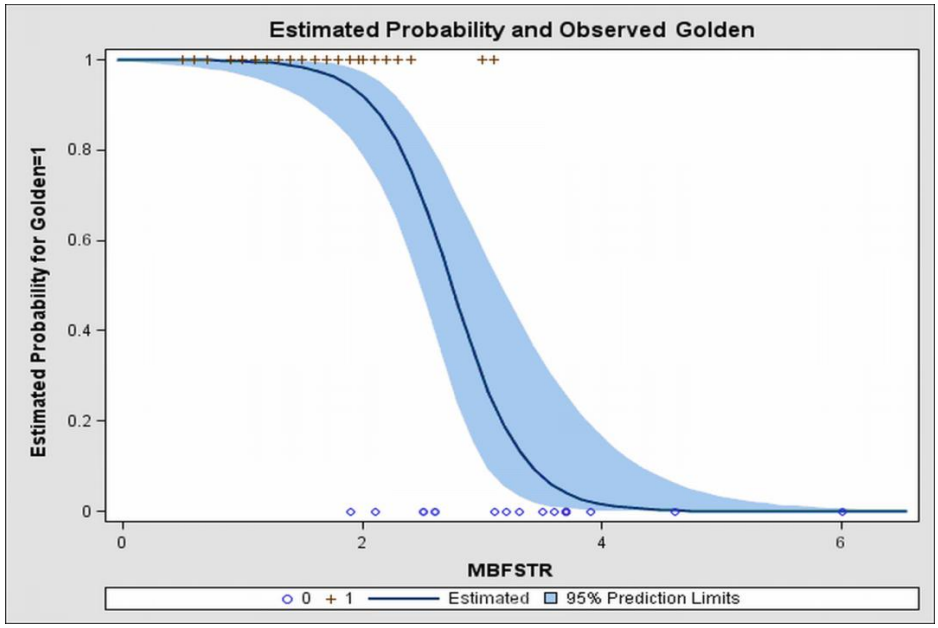

Panel d

Figure 15: ROC analysis of myocardial regions with significant stenoses in CT angiography. **Panel a**: ROC curve of PET perfusion against gold standard with cut-off values. **Panel b**: Estimated probability of significant CAD against stress MBF. MBFSTR=stress MBF; Golden=ICA and FFR.

Figures 16, 17 and 18 demonstrate patient cases that reflect the power of hybrid imaging. In **Figure 16**, anatomically significant stenoses are not accompanied by reduced perfusion whereas **Figure 17** exhibits significant stenoses both by means of anatomy and by impaired flow. **Figure 18** shows a case in which epicardial vessels are non-stenotic but perfusion is impaired because of presumed small vessel disease.

Figure 16, panel 1

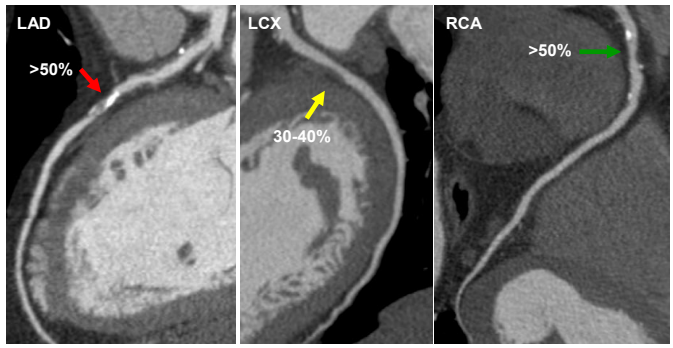

Figure 16, panel 2

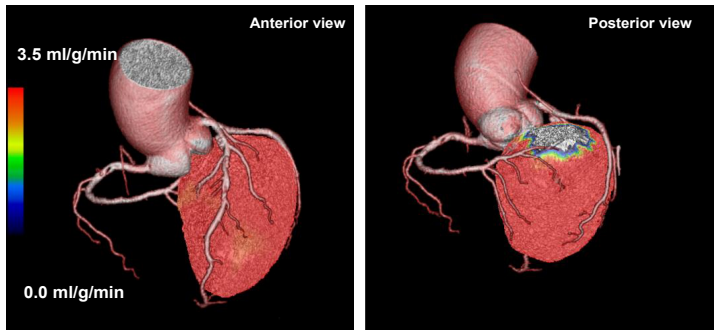

Figure 16, panel 3

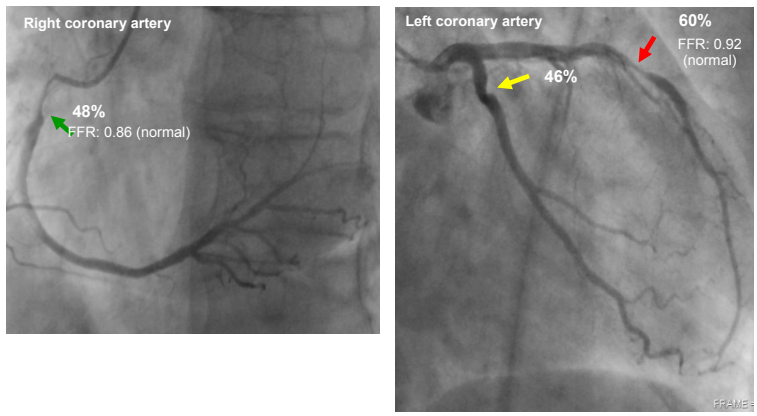

Figure 16: Findings in a 69-year-old male with impaired glucose tolerance, arrhythmias and attacks of anginal pain. The patient had moderately reduced exercise capacity and atypical pain with <1 mm ST depression in exercise ECG. **Panel 1**: CTA showed significant stenoses in LAD and RCA while only mild stenosis was present in LCX. **Panel 2**: Hybrid images displayed with stress PET perfusion coloring the surface of left ventricular wall (absolute scale 0-3.5 ml/g/min). Normal perfusion is above 2.5 ml/g/min (yellow or red color). In this patient stress perfusion was normal in all regions. **Panel 3:** ICA with quantitative analysis and FFR. Despite anatomically significant narrowing of LAD and borderline changes in RCA, FFR was normal in both vessels indicating functionally non-significant disease.

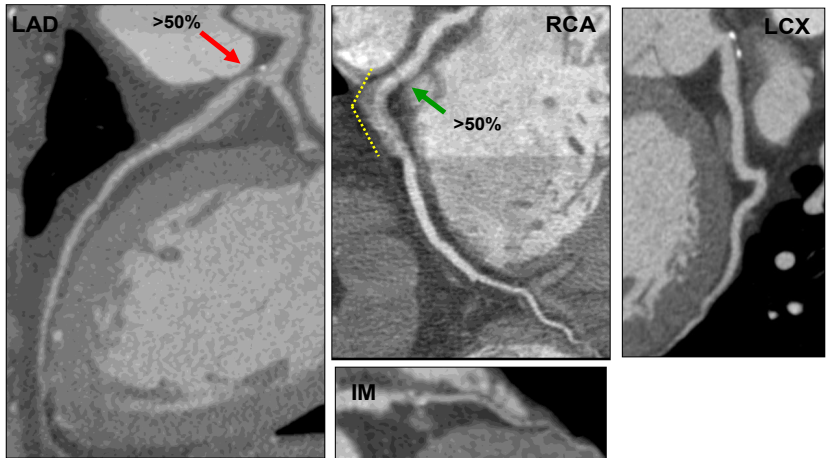

Figure 17, panel 1

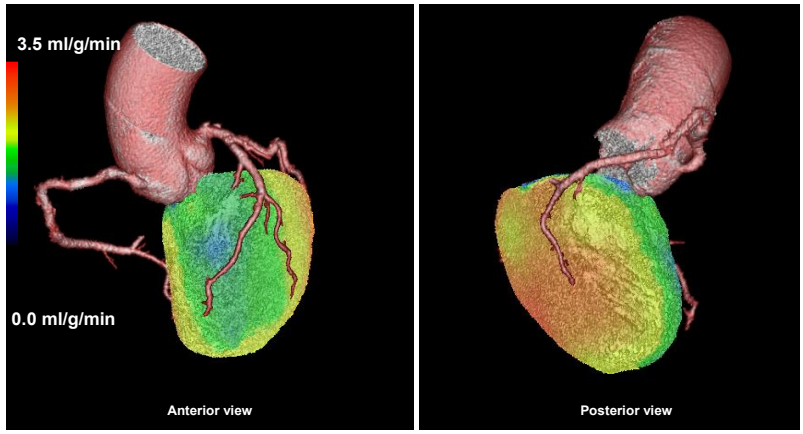

Figure 17, panel 2

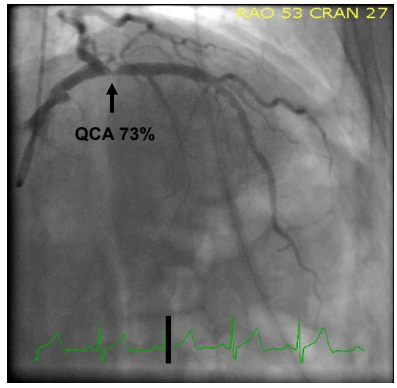

Figure 17, panel 3

Figure 17: An example of findings in a 57-year-old male with hypertension and hyperlipidemia. He suffered from atypical chest pain during exertion. In exercise test he had good performance, no symptoms but 1 mm ST depression in ECG. **Panel 1**: CT angiography curved multiplanar reconstructions of the major coronary vessels show significant stenoses in LAD, RCA and in a small intermediate branch (IM). LCX was not stenosed. Yellow dotted line denotes motion artifacts in RCA. **Panel 2**: Hybrid volume rendered image. Stress myocardial perfusion was reduced in the area supplied by LAD. In all other regions perfusion was normal. **Panel 3:** Invasive angiography with quantitative analysis showed significant 73% luminal narrowing in LAD. Other vessels were non-stenosed.

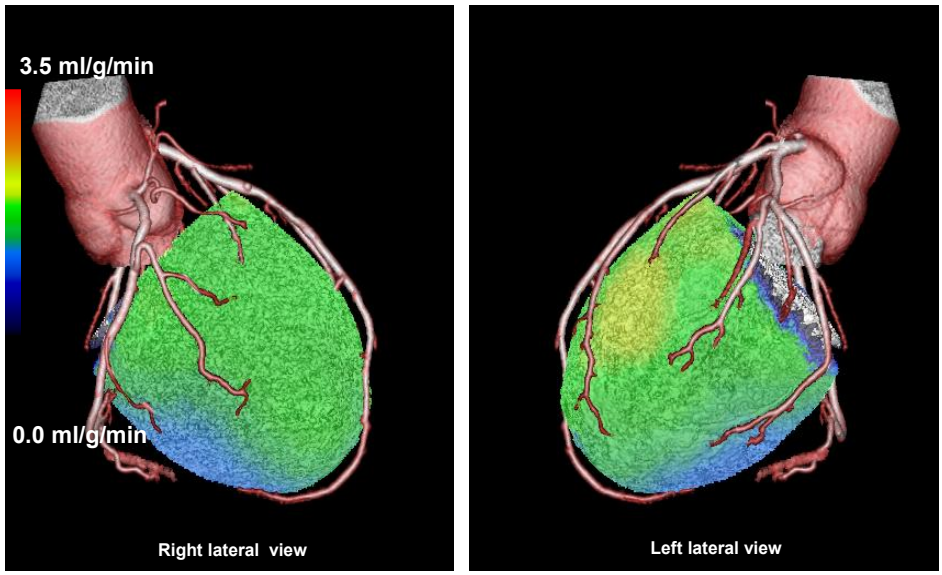

Figure 18: **A 63-year-old male with a family history as a risk factor for CAD and atypical chest pain during exertion**. Good performance in exercise test, However atypical chest pain and 2 mm ST depression in ECG. Hybrid volume rendered images show that stress myocardial perfusion was reduced in most regions (green and blue color). However, both CT and invasive angiographies showed normal coronary arteries indicating that the cause of perfusion abnormalities is other than epicardial disease - possibly micro- vascular disease.

5.5. Absolute Quantification of Myocardial Perfusion (Study V)

According to the gold standard, 40/104 patients had significant CAD. Of these, 25 had multi-vessel disease and 15 single-vessel disease. The data was re-evaluated after the hybrid PET/CT analysis of study IV, which changed the categorization of 2 borderline patients from having single-vessel disease to having actually multi-vessel disease.

Patient-based analysis

In patient based analysis, when the images were evaluated *visually*, sensitivity was 87% and specificity 86% for the assessment of the images scaled according to absolute flow. When the scale was relative, sensitivity climbed to 92% at the cost of specificity which was only 40%. The positive predictive values (PPVs) were 79% for absolute evaluation and 48% for images scaled to relative flow; the negative predictive values (NPVs) were 92% and 90%, respectively.

In *numerical* analysis of the absolute flow, patient-based sensitivity was 95%, specificity 91%, PPV 86% and NPV 97%. In the numerical analysis of the relative flow, sensitivity was only 76% and specificity 71%. PPV was 60% and NPV 84%. The results of the patient-based analysis are exhibited in **Figure 19**.

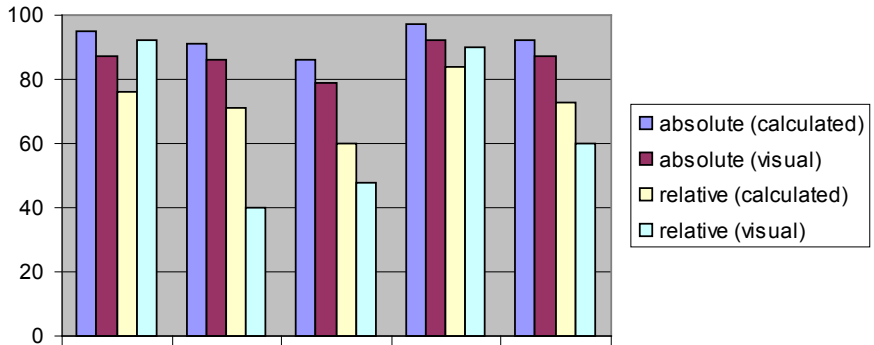

	Sensitivity (%)	Specificity (%)	PPV (%)	NPV (%)	Accuracy (%)
absolute (calculated)	95	91	86	97	92
absolute (visual)	87	86	79	92	87
relative (calculated)	76	71	60	84	73
relative (visual)	92	40	48	90	60

Figure 19. Patient-based comparison of assessment methods in significant CAD: Absolute quantification and relative assessment of stress perfusion against gold standard (invasive angiography and fractional flow reserve). *Absolute calculated* (blue bar): assessment of MBF using numeric values and a preset cut-off point. *Absolute visual* (burgundy bar) visual assessment of absolute flow in hybrid images with a preset absolute color scale. *Relative calculated* (yellow bar): assessment of relative differences in perfusion when converted into numerical data. *Relative visual* (light blue bar): visual assessment of relative differences in perfusion in hybrid images. N=104.

Of the 25 patients with *multi-vessel disease*, 24 underwent PET. All but 1 was correctly identified with absolute quantification of the stress perfusion when numerical flow values were employed; 1 was a false negative. Using visual-only absolute quantification of multi-vessel disease, 3 cases of the 24 were false negatives. With both techniques of absolute quantification, there were 5 false positives for multi-vessel disease. Each had diffusely reduced MBF with no significant CAD according to ICA/FFR.

With relative analysis, we were able to assess only 9 of the 24 patients with 3-vessel disease correctly. 2 patients were erroneously interpreted as being normal (both had very low but diffusely reduced flow) whereas the remaining 13 were thought to have 1-vessel disease only. In addition, 26 patients were classified as having 3-vessel disease although they did not; 19 of them had actually no significant disease at all whereas 7 had 1-vessel disease instead. The results of the analysis of patients with multi-vessel disease are presented in **Figure 20.**

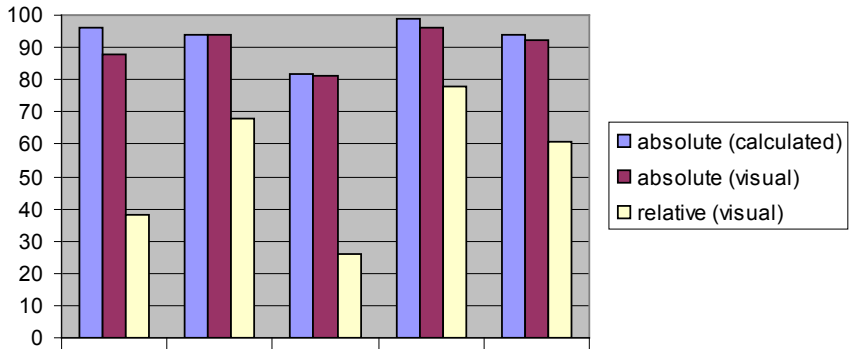

	Sensitivity (%)	Specificity (%)	PPV (%)	NPV (%)	Accuracy (%)
absolute (calculated)	96	94	82	99	94
absolute (visual)	88	94	81	96	92
relative (visual)	38	68	26	78	61

Figure 20. Analysis of patients with multi-vessel disease: Absolute quantification and relative assessment of stress perfusion against gold standard (invasive angiography and fractional flow reserve). *Absolute calculated* (blue bar): assessment of MBF using numeric values and a preset cut-off point. *Absolute visual* (burgundy bar) assessment of "absolute" flow by visual examination of hybrid images with a preset absolute color scale. *Relative perfusion* (yellow bar): visual assessment of relative differences in perfusion in hybrid images. N=104.

For further classification, the patients were categorized into groups according to the clinical performance of the image-based analysis methods. First, the group of no major difference in clinical interpretation consisted of 60 patients, 59% of the subjects. This group included studies that were correctly diagnosed as abnormal with both methods (n=31), correctly diagnosed as normal with both techniques (n=22), as well as those in which neither method was able to give the right diagnosis (n=7). 36 patients (34%) had heterogeneous and thus abnormal relative perfusion but their absolute perfusion was normal. There were 15 patients in whom the relative analysis missed the correct diagnosis of significant multi-vessel disease. Although most cases could be correctly identified using quantification, there was interestingly 1 patient with correct diagnosis of multi-vessel disease at relative analysis but with a false negative result when images with quantification were used.

Region-based analysis

In *regional* (vessel-based) analysis using *visual relative* assessment of the perfusion images, the PPV was 39%, the NPV 85% and the accuracy 68% while the sensitivity and the specificity were 60% and 79%, respectively. The PPV, NPV and accuracy of absolute perfusion in the detection of significant CAD were 70%, 90% and 86%, respectively, while the sensitivity and the specificity were 69% and 90%, respectively. When the visual assessment was replaced by the analysis of the

numerical values of the absolute flow, the PPV, NPV and accuracy improved to 78%, 98% and 92%, respectively, while the sensitivity was 95% and the specificity 92%. These results of the absolute numerical values were, in addition, compared to those obtained by the relative values by means of ROC analysis. The area under the curve was 0.9447 (absolute analysis) and 0.7335 (relative analysis). The optimal cut-off for the absolute analysis was determined as 2.5 and the relative analysis as 0.8 on the basis of the ROC curve. The region-based results are presented in **Figures 21-22.**

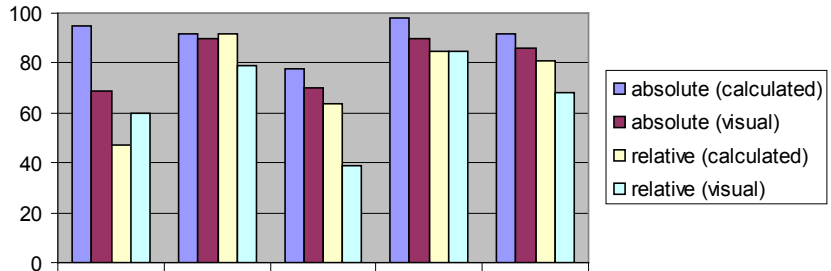

	Sensitivity (%)	Specificity (%)	PPV (%)	NPV (%)	Accuracy (%)
absolute (calculated)	95	92	78	98	92
absolute (visual)	69	90	70	90	86
relative (calculated)	47	92	64	85	81
relative (visual)	60	79	39	85	68

Figure 21. Region-based comparison of assessment methods in significant CAD: absolute quantification and relative assessment of stress perfusion against gold standard (invasive angiography and fractional flow reserve). *Absolute calculated* (blue bar): assessment of MBF using numeric values and a preset cut-off point. *Absolute visual* (burgundy bar) visual assessment of absolute flow in hybrid images with a preset absolute color scale. *Relative calculated* (yellow bar): assessment of relative differences in perfusion when converted into numerical data. *Relative visual* (light blue bar): visual assessment of relative differences in perfusion in hybrid images. N=312.

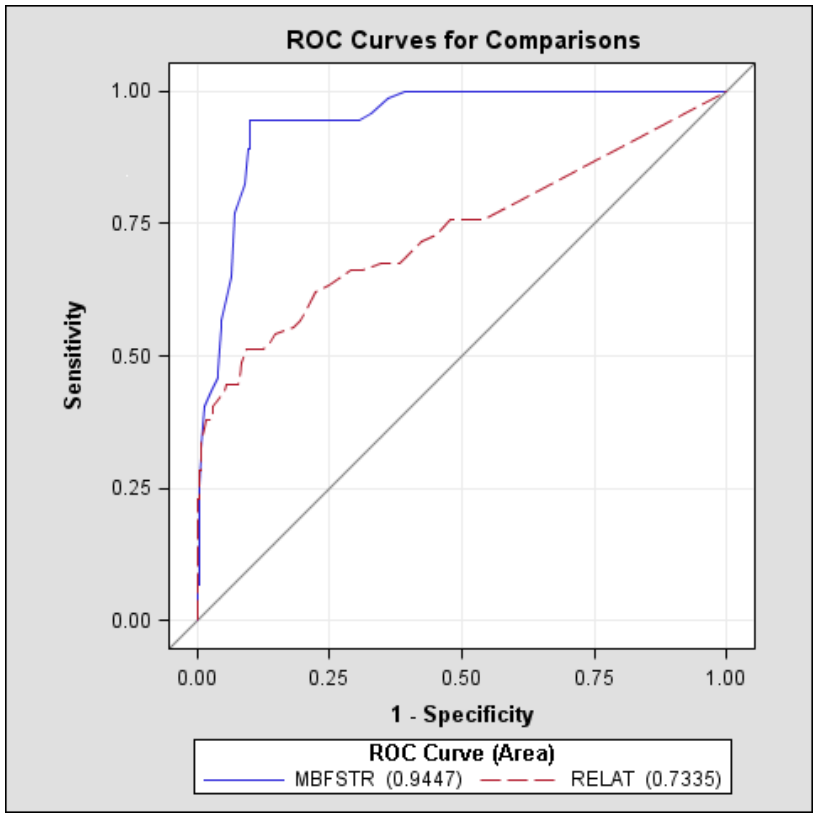

Figure 22. ROC curves of absolute and relative myocardial blood flow vs. reference (invasive angiography with FFR) in adenosine-induced stress. Solid blue line: absolute flow. Dotted red line: relative flow. MBFSTR, stress myocardial perfusion in absolute terms; RELAT, stress relative perfusion

6. DISCUSSION

The results of Study I show that a comprehensive non-invasive imaging of both coronary angiography and rest-stress myocardial perfusion can be performed with radiation dose <10 mSv in a vast majority of patients. The results also suggest that both the image quality and clinical confidence of MDCT is preserved despite significant reduction in radiation dose.

Due to improved accuracy, the number of coronary CT scans is growing rapidly and is expected to increase (Berman, *et al* 2006; Einstein, *et al* 2007). Although the mean radiation dose of 64 MDCT cardiac studies has recently been estimated as 15.2 mSv for males and 21.4 mSv for females (de Feyter, *et al* 2007), there is probably wide variation of radiation doses received by the patients in daily practice and individual doses may even be up to 40 mSv (Paul & Abada 2007). Skin, breast, oesophagus and heart have the highest recorded absorbed organ doses. Of particular concern is the female breast that may receive a dose 10-30 times higher than received by mammography screening (Nickoloff & Alderson 2007). In fact, the relative risk for breast cancer incidence for girls and women is estimated to be 1.004–1.042 for a single examination (Hurwitz, *et al.* 2007). In comparison, diagnostic ICA has a mean effective radiation dose of 2.5–5 mSv, and nuclear perfusion imaging with SPECT has a mean effective radiation dose of ~ 15–20 mSv (Einstein, *et al* 2007).

The primary ways to avoid unnecessary radiation are proper and careful patient selection (including adequate indications for the study) and preparation. Although data from high-probability patients is still scarce, it seems that CTA is most suitable for low to medium risk groups. Dense coronary calcifications deteriorate image quality and it has been stipulated that patients with very high calcium scores should be omitted from CTA in favour of other methods. Massive obesity tends to degrade image quality. Patient preparation should be optimized including adequate heart rate control if necessary. Accordingly, our data show that imaging with high heart rates often produce poor images.

Classic methods to decrease radiation dose by reducing tube current and voltage and increasing the pitch are widely used - but compromise image quality at least to a certain degree. Anatomy based current modulation (either real time or scout image based) depends on tissue attenuation; the more attenuating tissue there is in the field of view the more radiation is used. An even more sophisticated method, ECG-dependent X-ray tube current modulation, reduces current only at phases outside the critical time window between end systole and end diastole (Kalender, *et al.* 1999; Morin, *et al* 2003; Prinak, *et al.* 2006; Fei, *et al* 2007).

Our approach, sequential step-and-shoot imaging with prospective ECG-triggering, utilizes existing hardware and is essentially a modification of traditional axial imaging adapted to a wide MDCT detector. While being a very efficient way to reduce dose, the additional advantage of this technique is the relative ease of implementation: it is a software add-on that can be used with existing scanners including some hybrid PET/CT models. While this technique may offer diagnostic CTA at doses as low as 1-2 mSv (Husmann, *et al* 2008), we chose to use the mode with a wider time window (125-200 msec) to ensure uncompromised image quality using a novel imaging method. Even so, the technique reduced dose by more than 60% as compared to spiral imaging with similar current, slice thickness and voltage. Further narrowing of the time window ("padding") will result in further dose reduction and should be considered in clinical protocols especially on patients with a low and stable HR.

In addition to the inability to scan patients with high or unstable heart rates, there appears to be just a single main limitation using the sequential technique, namely the lack of information from phases outside the predetermined time window. In contrast to ECG-modulated spiral imaging, the step-and-shoot technique does not provide images of every phase of the R-R-interval, thus disabling the evaluation cardiac motion and functional measures such as ejection fraction. In clinical practice, such occasions seem to be rather scarce.

The principle limitation of the first part of study I was the lack of anatomical reference such as catheter angiography to confirm the image quality of the images. The performance of spiral 64-sector coronary MDCT however, is now reasonably well established. While statistically non-significant, difference between average heart rates between the two groups may have had effect on image quality. Another major, though in our opinion unavoidable limitation is that the reader cannot work completely blinded to the protocol used due to obvious signs in images such as more visible change in contrast media concentration between the image stacks in sequential data sets.

Although reports indicate that females receive higher effective doses from coronary CT than males, we did not select patients on the base of their gender. This may have exaggerated the variation of dose between the groups in the first part. Based on the literature, however, it is unlikely that this difference is big enough to explain but a minor fraction of the reduction.

Study II is one of the first studies using anatomical assessment of the coronary arteries to examine the prevalence of CAD among patients with paroxysmal or persistent AF (and without a history of CAD). A higher prevalence of obstructive CAD was detected among the AF patients, as compared to a cohort of patients without AF, with similar age and pre-test likelihood of CAD, but with a higher prevalence of diabetes mellitus. In addition, LM and/or proximal LAD disease was

more frequently identified in AF patients (25%) than in non-AF patients (10%). AF, together with age and male gender, was identified as an independent predictor of the presence of obstructive CAD.

Although a causal relationship between CAD and AF has not yet been established, CAD is considered to be highly prevalent among patients with AF and may be one of its potential etiological factors. AF and CAD may simply be different, concurrent consequences of long-lasting exposure to coronary risk factors, but, on the other hand, AF could be a consequence of CAD, directly or indirectly, through an increase of left atrial pressure secondary to episodes of left ventricular ischaemia. Previous population studies reported CAD to be one of the etiological factors most commonly associated with the development of AF. Once diagnosed with AF, the presence of CAD has been shown to be related with recurrent AF episodes, presence of symptoms (including arrhythmic, heart failure and angina symptoms) and increased risk of death. Epidemiologic data disclosed that ischemic heart disease is one of the most common underlying cause of death among AF patients. These observations have lead to an increased interest in the imaging of CAD in patients with AF.

In the present study, imaging of atherosclerosis with CT was used to determine the prevalence of CAD. By means of calcium scoring, the presence and extensions of coronary calcifications was not statistically different between AF and non-AF patients. However, using CTA, AF patients were found to have more frequently coronary atherosclerosis (82%) and obstructive CAD (41%), as compared to non-AF patients (68% and 27%, respectively). These findings are important when considering the fact that the patients were mostly asymptomatic and with low pre-test likelihood for CAD. In addition, a higher prevalence of diabetes, a condition that is generally associated with a high extent of CAD, was observed in non-AF patients. Indeed, only AF, age and male gender were identified as significantly related to the presence of obstructive CAD.

In study III we assessed the reproducibility of a novel cardiac PET analysis software, Carimas™, for the analysis of ^{15}O-water myocardial perfusion (MP) studies. Four observers with various experience levels evaluated 20 real clinical MP studies, repeating each analysis twice. We found that Carimas™ can reliably quantify MP in a whole heart but also in coronary artery regions and in standardized myocardial segments. The analysis was found to be robust enough even for the less experienced observers but the best results were obtained when analysis was done by the experienced nuclear medicine specialist. The preliminary clinical accuracy, although in a small patient population, was also excellent. No one, to our knowledge, has yet assessed the myocardial perfusion reproducibility in the same methodological framework (new software – ^{15}O-water – several observers – linear mixed model) as we have.

Our findings suggest that Carimas™ provides good reproducibility for absolute quantification of myocardial perfusion. When global perfusion was analyzed, excellent reproducibility was found independently of the observer's experience. The intra-observer difference was close to zero, the most prominent being 9.9% during stress in the least experienced observer. The inter-observer difference was also very small (8.5%). When analyzing the reproducibility on the regional and segmental levels, the best results were detected in the most experienced observer but they were very good also in the less experienced readers. The most consistent differences were found in the novice observer analysing the stress images. Even then, the intra-observer difference was not higher than 14.3% and the difference between the most and the least experienced observers was only 12.1%.

The most difficult region to evaluate seems to be the basal segments of the septal wall. This is comprehensible because it is due to the variability of the septal length causing problems for the definition of septal ROIs. The variation in heart axis definition may also have a greater impact on the smaller-sized ROIs. Despite these facts the reproducibility even in these regions was reasonably good.

^{15}O-water has been regarded as the most challenging perfusion tracer for clinical applications because it does not produce immediate image of perfusion distribution. In study III, we tested the method in small group of patients with moderate likelihood of CAD, and found that the accuracy of quantitative perfusion was excellent. The cut-off value of 2.5 mL/g/min established in study III was reconfirmed in study IV with a larger patient population. In Carimas™, no new modelling is implemented. Rather, image processing, segmentation and ROI definition were improved to allow a more accurate regional analysis of MP in clinical situations.

Study IV investigated the power of hybrid imaging in the detection of CAD. No large clinical study has previously provided a direct comparison between non-invasive and invasive imaging that combine anatomy and function. In this prospective study, 107 patients with symptoms suggestive for CAD were investigated using a novel imaging technique, hybrid PET/CT. The study has several unique properties: 1) it is the first study to take full advantage of both CTA and PET perfusion imaging and was performed using a hybrid imaging device; 2) it included quantitative analysis; 3) the patients had moderate pre-test likelihood of CAD (a clinically appropriate population); 4) all patients entered invasive tests independently of the non-invasive imaging results to avoid referral bias, and; 5) the combination of ICA and FFR was used as reference.

Our results show that non-invasive hybrid PET/CT imaging is a superb diagnostic method for the comprehensive diagnosis of CAD and its severity, and may be performed routinely using a short, low radiation dose protocol. CTA alone can rule out significant CAD with an extremely high NPV (97% per patient and 94%

per vessel). On the other hand, it is difficult to accurately evaluate the degree of stenoses detected. This problem has been demonstrated in a number of studies and results in modest PPV in comparison to ICA. Second, even when the degree of anatomical lesions is accurately detected, it is difficult to estimate the functional significance of borderline stenoses. This handicap is inherent in all anatomical imaging.

PET perfusion imaging is also able to rule out significant CAD with an extremely high NPV (97% per patient and 98% per vessel). Thus, normal perfusion indicates the presence of no hemodynamically compromising CAD. Reduced perfusion, however, may mean not only significant epicardial disease, but also the presence of micro-vascular abnormalities. These changes increase the risk for cardiac events but are difficult to distinguish from epicardial disease by measuring perfusion alone. Our results of PPV of 86% (78% per vessel) suggest that there was a considerable amount of small-vessel disease present in this patient population.

We employed absolute quantification of MP while the traditional clinical method is to identify relative inducible perfusion defects during stress. Until now, the absolute quantification using PET has rarely been employed in clinical studies. Our ROC analysis shows that the optimal cut-off between normal and pathological MBF is <2.5 mL/g/min in stress, confirming our preliminary findings from study III. Practically all regions with MBF <2.0 mL/g/min were abnormal, suggesting that MBF between 2.0 and 2.5 can be considered mildly abnormal and values <2.0 clearly abnormal.

This study demonstrates the power of hybrid PET/CT imaging combining both anatomy and function. When MP is restricted, CT angiography can demonstrate the degree and location of stenosis and separate micro-vascular from epicardial disease. When CTA shows coronary plaques, possible perfusion deficits can be related to their epicardial locations. In our study, the accuracy of the hybrid technique was excellent.

We used ^{15}O-water as a perfusion tracer. This tracer is not widely available because it requires an on-site cyclotron. However, other validated tracers such as ^{13}N-ammonia and ^{82}Rubidium or novel ^{18}Fluorine labeled tracers are likely to provide comparable results if proper protocols and quantification are applied. In the recent study by El Fakhri, *et al* (2008), MBF obtained with ^{82}Rubidium was comparable to that of ^{13}N-ammonia with a slight tendency to underestimate MBF during stress. ^{82}Rubidium can easily be distributed to clinical sites without own tracer production laboratory which may facilitate the wider distribution of the technique into clinical routine.

In the current protocol, we performed CTA before PET because we plan to avoid perfusion imaging in clinical routine if CTA is normal. Another reason for the “CT first”-approach is its ability to detect and characterize plaques even when they

are not flow-limiting. It is important to assess these changes to warrant suitable medication. Although we did not perform the cost-benefit analysis, it is likely that such a protocol is efficient because the cost of a CTA exam is lower than that of a PET study, and about half of the patients undergoing CTA will not require perfusion imaging in an appropriate population.

Beta blockers were used in most of the patients prior to imaging. Theoretically this could reduce the sensitivity of perfusion imaging which seems, however, not to be a problem since the sensitivity of PET was excellent. Combining two techniques that both utilize radiation will obviously increase the radiation dose. However, as in study I, we found that novel CT techniques reduce the dose considerably. The dose from PET, on the other hand, is only a fraction of doses in SPECT and can be further reduced by performing stress imaging only. Same applies if one chooses a "PET first" protocol and performs CT only to those patients with impaired MBF.

In study V we further investigated the clinical value of absolute quantification of MBF. In certain clinical situations, estimates of relative differences in perfusion may not be sufficient for accurate diagnosis. In this study, we compared this "conventional approach" to the approach of measuring the absolute myocardial flow.

There are at least 3 major scenarios in which the differences between relative and absolute perfusion may be particularly important. First, with relative analysis we would have totally missed 2 patients with 3-vessel disease and balanced reduction of perfusion because diffusely reduced flow was uniform and visually homogenous. This is a previously known phenomenon and has important diagnostic and prognostic consequences. Using absolute quantification, however, it is usually easily distinguished from normal perfusion.

The second group of patients with numerous discrepancies between the absolute and relative analysis methods were other patients with multi-vessel disease. 13 patients were incorrectly labeled as having only single-vessel disease in relative perfusion analysis of images. This, too, is easy to understand because the region with the best perfusion is considered to represent normal flow in relative analysis - which is however not usually the case in patients with multi-vessel disease.

Third, visual analysis of relative flow resulted in a large group of patients with inhomogeneous perfusion that was classified as abnormal but that was actually shown to be quantitatively high albeit slightly heterogeneous. According to the reference method (ICA with FFR), these patients had no significant CAD. Part of this relative heterogeneity of the flow is probably attributed to the physiological variance of normal high flow. This phenomenon is exposed when using tracers with linear relationship between the measured and actual flow up to very high flow values, such as ^{15}O-water. Yet, with any tracer it is possible that slight colour variances within myocardium are prone to be diagnosed as "possible" or

"probable" ischemia. This phenomenon is well known from SPECT imaging, in which it is common practice to categorize the findings into several groups by the certainty of the disease.

Another important subgroup is the patients with normal (or nearly normal) epicardial vessels (i.e. showing no stenoses) but with diffusely reduced perfusion. This implication of probable microcirculatory deficiency may readily be visualized using absolute quantification but, analogous to the evaluation of the multi-vessel disease, is frequently missed when just relative perfusion abnormalities are assessed. Of course, the relative quantity of patients with multi- and single vessel disease as well as impaired microcirculation reflects a particular patient population and the pre-test probability of CAD in that group.

The poor performance of relative analysis at high perfusion range using ^{15}O-water should not be directly extrapolated to other PET tracers without quantification or tracers used in conventional nuclear medicine. Most tracers (such as sestamibi, tetrofosmin, ammonia and rubidium) exhibit non-linear flow characteristics between detected signal and actual perfusion, thus naturally omitting heterogeneity in perfusion at the high end of the normal perfusion range, as demonstrated in **Figure 23.**

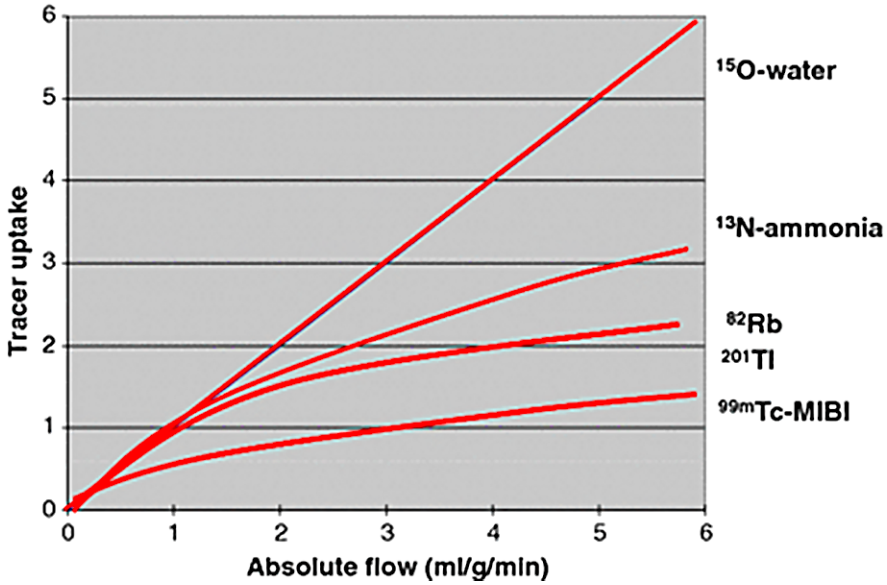

Figure 23. Graphical presentation of the relationship between absolute myocardial perfusion and tracer uptake. The lines are estimates of the tracer uptake characteristics. In all tracers except 15O-water, tracer extraction is reduced when perfusion is increased. (Reproduced with permission (ref: Knuuti J, Kajander S, Mäki M, Ukkonen H. Quantification of myocardial blood flow will reform the detection of CAD. J Nucl Cardiol. 2009;16:497-506. Epub 2009 Jun 3.)

Using ^{15}O-water by definition and with other tracers after quantification, the normal variation of perfusion is large and must be taken into account in the interpretation. The simplest solution is to use a fixed absolute scale in the images: the brightest color will be assigned to certain absolute level of perfusion (e.g. 3.5 mL/g/min) to enable easy detection of change from normal to reduced perfusion (e.g. at 2.5 mL/g/min) at which the color will change from yellow to green in rainbow scale.

In the comparison between quantification and relative assessment we utilized visual hybrid PET/CT images with a straight forward normal/abnormal scale. We used these images for visual evaluation instead of the more conventional "bulls eye"-type ones or slice analysis traditionally used in nuclear medicine. The strategy was chosen because if offers visualization of the actual vessels and their territories in an individual basis. The normal variation in anatomy is considerable and possible "non-anatomical" pseudo lesions in perfusion images are more easily distinguished from real abnormalities. The accuracy of the quantification of the flow, however, seems to further improve by utilizing numerical values of the MBF instead just colours. The cut-off between abnormal and normal may then be optimized and the number of indeterminate results is likely to decrease. Based on our results, it is advisable to utilize hybrid images for anatomy and flow values for function if both are available.

In these studies, we have shown that it is possible to non-invasively but accurately characterize the existence and severity of CAD in a patient population that may be the most challenging: those people with a moderate pre-test probability to have CAD. Using absolute quantification, even the patient groups with notably difficult assessments, such as those with balanced triple-vessel disease, may be correctly evaluated.

With the combination of CTA and PET perfusion, we can reach the correct diagnosis with a moderate radiation dose and a short protocol that is feasible in clinical, day-to-day use.

7. CONCLUSIONS

The following conclusions may be drawn from the studies presented in this thesis.

I Low dose PET/CT with sequential acquisition and prospective ECG-triggering allows cardiac hybrid studies with radiation dose less than 10 mSv. The protocol can be applied to almost 9 out of 10 patients with CT image quality comparable to the more commonly used spiral acquisition.

II Higher prevalence of CAD is associated to AF when comparing coronary CTA to sinus rhythm.

III Excellent reproducibility of the quantification of MP with ^{15}O-water PET can be reached when analyzed by Carimas™ software. The results support the good clinical value of the software.

IV Cardiac hybrid PET/CT imaging allows accurate non-invasive detection of CAD in a population with intermediate pre-test likelihood to have CAD. The method is feasible and can be routinely performed with <10mSv radiation dose in most patients.

V Absolute measurement of MP has significant impact on the interpretation of myocardial perfusion studies. In particular, quantification is able to correct the regional variances within normal flow. In addition, multi-vessel disease is more accurately detected. Visual analysis of the images should be complemented with the assessment of the actual flow values.

8. ACKNOWLEDGEMENTS

This work was carried out at the Turku PET Centre during the years 2007-2010. I am grateful for having been able to work in such a dynamic, inspiring and, sometimes, even truly hilarious community.

I want to express my gratitude in particular to Juhani Knuuti, my supervisor, for inspiring me to take part in research after several years of clinical radiology. It has been a challenging but also a rewarding task to train the old brain – and to see that science may also be fun. Together with Heikki Ukkonen, we started the clinical routine for coronary CT in 2005, soon to be coupled with cardiac PET. These experiences, eventually, ignited the research that made this thesis possible. Multimodality imaging, if anything, is team work. The newer additions to the group, Esa Joutsiniemi, Antti Saraste and Jussi Pärkkä have brought youthful energy to the team. The more experienced energy comes from the senior members of the group, Markku Saraste, Juhani Airaksinen and Jaakko Hartiala. Last but definitely not least, Maija Mäki has been my best possible tutor in cardiac PET.

I was first introduced to clnical PET by Marko Seppänen when we switched jobs in 2004-5. It has always been rewarding and fun to work with Marko and I have learned a lot through him. Recently, Jukka Kemppainen has adopted the role of my “clinical team mate” in PET imaging with equal success. Terhi Tuokkola has been not only an excellent colleague in radiology but also a great help in patient studies while I have been absent from my clinical post.

Discussions with Mika Teräs have not always concentrated on the subject of cardiac imaging. Rather, they have fluctuated between world economy, sports and politics – a combination that is definitely good for the mental health. Hannu Sipilä, the wizard behind O15-production, has also been a great companion in coffee-table discussions.

Heikki Minn, with his vast knowledge on PET (and birds, for that matter), has always been an invaluable mentor - and another person to share with the most recent information on sports.

Also, I want to thank Pirjo Nuutila and Juha Rinne for their support. Virva Lepomäki, with her knowledge and enthusiasm for MRI and cooking, has been the best possible person to share a room with. Tuula Tolvanen and Tommi Noponen have been of great help in understanding physics. Well, at least a little bit of it.

Rami Mikkola and Marko Tättäläinen provided great expertise on IT. Chunley Han, the father of my godson, is the brain behind Carimas, and thus one of the key persons in this study along with Serge Nesterov. Ville Aalto assisted in a crucial matter, the statistics.

My special thanks must go to the radiographers at the PET Centre. Co-operation has been seamless and the imaging sessions – quite often – even fun. Tarja Keskitalo, Marjo Tähti, Minna Aatsinki, Anne-Mari Jokinen, Heidi Betlehem, Hannele Lehtinen and Kaleva Mölsä: thank you!, Equal appreciation goes to medical laboratory technologists Sanna Suominen, Heidi Partanen, Emilia Puhakka, Eija Nirhamo, Leena Tokoi and Minna Tuominen: even I learned to use the (very simple) radiowater injection system under your guidance.

I also warmly thank Sinikka Lehtola and Mirja Jyrkinen for the always important secretarial matters. Without them these studies simply would not have been done.

I am grateful to Marja Hedman and Stephen Schroeder who served as the official reviewers of the thesis. Seppo Koskinen and Petri Sipola took part in the guidance group of the work.

I do not want to forget my background in clinical radiology and I want to thank all the colleagues that I have worked with during the past years. It was there I learned the basics of medical imaging.

I have a circle of friends that have always supported me. Without their help, this task would have been much more difficult, if not impossible.

I want to thank my parents, Eeva and Aaro, as well as my brother Sakari for the continuous and invaluable support that I have received through the years. I could not have hoped for a better home when I grew up.

Life would have been so much more difficult and boring without my dear wife Jaana and sons Samuli, Santeri and Oskari. You have provided me with love, passion and the newest family addition, Onni the Labrador. Jasu, thank you for holding the family together also in difficult times. ❤

Sami Kajander

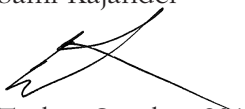

Turku, October 2010

9. REFERENCES

1. Abada HT, Larchez C, Daoud B, Sigal-Cinqualbre A, Paul JF. MDCT of the coronary arteries: feasibility of low-dose CT with ECG-pulsed tube current modulation to reduce radiation dose. *Am J Roentgenol.* 2006;186:387-90.

2. Abdulla J, Abildstrom SZ, Gotzsche O, Christensen E, Kober L, Torp-Pedersen C. 64-multislice detector computed tomography coronary angiography as potential alternative to conventional coronary angiography: a systematic review and meta-analysis. *Eur Heart J* 2007;28:3042-50.

3. Abidov A, Hachamovitch R, Rozanski A, Hayes SW, Santos MM, Sciammarella MG, Cohen I, Gerlach J, Friedman JD, Germano G, Berman DS. Prognostic implications of atrial fibrillation in patients undergoing myocardial perfusion single-photon emission computed tomography. *J Am Coll Cardiol* 2004;44:1062-70.

4. Ambrose J. Computerized transverse axial scanning (tomography) 2, *Br J Radiol* 1973;46:1023-47.

5. American Heart Association. *Heart disease and stroke statistics – 2004 update*. Dallas, Texas: American Heart Association, 2003.

6. Anagnostopoulos C, Almonacid A, El Fakhri G, Curillova Z, Sitek A, Roughton M, Dorbala S, Popma JJ, Di Carli MF. Quantitative relationship between coronary vasodilator reserve assessed by 82Rb PET imaging and coronary artery stenosis severity. *Eur J Nucl Med Mol Imaging* 2008;35:1593-601.

7. Arias E, Anderson RN, Kung HC, Murphy SL, Kochanek KD. Deaths: final data for 2001. *Natl Vital Stat Rep* 2003;52:1–115.

8. Askew JW, Miller TD, Hodge DO, Gibbons RJ. The value of myocardial perfusion single-photon emission computed tomography in screening asymptomatic patients with atrial fibrillation for coronary artery disease. *JAm Coll Cardiol* 2007;50:1080-5.

9. Bateman TM, Heller GV, McGhie AI, Courter SA, Golub RA, Case JA, Cullom SJ. Multicenter investigation comparing a highly efficient half-time stress-only attenuation correction approach against standard rest-stress Tc-99m SPECT imaging. *J Nucl Cardiol.* 2009;16:726-35.

10. Bateman TM, Heller GV, McGhie AI, Friedman JD, Case JA, Bryngelson JR, Hertenstein GK, Moutray KL, Reid K, Cullom SJ. Diagnostic accuracy of rest/stress ECG-gated Rb-82 myocardial perfusion PET: comparison with ECG-gated Tc-99m sestamibi SPECT. *J Nucl Cardiol.* 2006;13:24-33.

11. Bax JJ, Beanlands RS, Klocke FJ, Knuuti J, Lammertsma AA, Schaefers MA, Schelbert HR, Von Schulthess GK, Shaw LJ, Yang GZ, Camici PG. Diagnostic and clinical perspectives of fusion imaging in cardiology: Is the total greater than the sum of its parts? *Heart* 2007;93:16-22.

12. Berger A, Botman KJ, MacCarthy PA, Wijns W, Bartunek J, Heyndrickx GR, Pijls NH, De Bruyne B. Long-term clinical outcome after fractional flow reserve-guided percutaneous coronary intervention in patients with multivessel disease. *J Am Coll Cardiol* 2005;46:438-42.

13. Bergmann SR, Fox KA, Rand AL, McElvany KD, Welch MJ, Markham J, Sobel BE. Quantification of regional myocardial blood flow *in vivo* with H215O. *Circulation* 1984;70:724-33.

14. Berman DL, Hachamovitch R, Shaw LJ, Friedman JD, Hayes SW, Thomson LE, Fieno DS, Germano G, Slomka P, Wong ND, Kang X, Rozanski A. Roles of nuclear cardiology, cardiac computed tomography and cardiac magnetic resonance: assessment of patients with suspected coronary artery disease. *J Nucl Med* 2006;47:74–82.

15. Berman DS, Wong ND, Gransar H, Miranda-Peats R, Dahlbeck J, Hayes SW, Friedman JD, Kang X, Polk D, Hachamovitch R, Shaw L, Rozanski A. Relationship between stress-induced myocardial ischemia and atherosclerosis measured by coronary calcium tomography, *J Am Coll Cardiol* 2004;44:923–30.

16. Beyer T, Townsend DW, Brun T, Kinahan PE, Charron M, Roddy R, Jerin J, Young J, Byars L, Nutt R. A combined PET/CT scanner for clinical oncology. *J Nucl Med.* 2000;41:1369-79.

17. Blue Cross and Blue Shield Association. Contrast-enhanced cardiac computed tomographic angiography in the diagnosis of coronary artery stenosis or for evaluation of acute chest pain. *TEC Asssesment* 2006;21.

18. Bol A, Melin JA, Vanoverschelde JL, Baudhuin T, Vogelaers D, De Pauw M, Michel C, Luxen A, Labar D, Cogneau M. Direct comparison of [13 N] ammonia and [15O]water estimates of perfusion with quantification of regional myocardial blood flow by microspheres. *Circulation* 1993;87:512-25.

19. Botman KJ, Pijls NH, Bech JW, Aarnoudse W, Peels K, van Straten B, Penn O, Michels HR, Bonnier H, Koolen JJ. Percutaneous coronary intervention or bypass surgery in multivessel disease? A tailored approach based on coronary

pressure measurement. *Catheter Cardiovasc Interv* 2004;63:184-91.

20. Boyd DP. A Proposed dynamic cardiac 3-D densitometer for early detection and evaluation of heart disease. *IEEE Trans Nucl Sci.*1979;26:2724.

21. Boyd DP, Couch JL, Napel SA, Peschmann KR, Rand RE. Ultrafast cine CT. Where have we been? What lies ahead? *Am J Card Imaging* 1987;1:175.

22. Budoff MJ, Achenbach S, Blumenthal RS, Carr JJ, Goldin JG, Greenland P, Guerci AD, Lima JA, Rader DJ, Rubin GD, Shaw LJ, Wiegers SE Assessment of coronary artery disease by cardiac computed tomography: a scientific statement from the American Heart Association Committee on Cardiovascular Imaging and Intervention, Council on Cardiovascular Radiology and Intervention, and Committee on Cardiac Imaging, Council on Clinical Cardiology. *Circulation* 2006;114:1761–91.

23. Castelli WP, Garrison RJ, Wilson PW, Abbott RD, Kalousdian S, Kannel WB. Incidence of coronary heart disease and lipoprotein cholesterol levels. The Framingham study. *JAMA* 1986;256:2835–8.

24. Cerqueira MD, Weissman NJ, Dilsizian V, Jacobs AK, Kaul S, Laskey WK, Pennell DJ, Rumberger JA, Ryan T, Verani MS. Standardized myocardial segmentation and nomenclature for tomographic imaging of the heart: a statement for healthcare professionals from the Cardiac Imaging Committee of the Council of Clinical Cardiology of the American Heart Association. *Circulation.* 2002;105:539-42.

25. Choi SI, George RT, Schuleri KH, Chun EJ, Lima JA, Lardo AC. Recent developments in wide-detector cardiac computed tomography. *Int J Cardiovasc Imaging* 2009; 25 Suppl 1:23-9.

26. Cormack A. Representation of function by its line integrals with some radiological applications. Part I. *J Appl. Phys* 1964;35:2722.

27. Cormack A. Representation of function by its line integrals with some radiological applications. Part II *J Appl. Phys* 1964;35:2908.

28. Dayanikli F, Grambow D, Muzik O, Mosca L, Rubenfire M, Schwaiger M. Early detection of abnormal coronary flow reserve in asymptomatic men at high risk for coronary artery disease using positron emission tomography. *Circulation.* 1994;90:808-17.

29. De Bruyne B, Baudhuin T, Melin JA, Pijls NH, Sys SU, Bol A, Paulus WJ, Heyndrickx GR, Wijns W. Coronary flow reserve calculated from pressure measurements in humans. Validation with positron emission tomography. *Circulation.* 1994;89:1013-22.

30. De Feyter PJ, Meijbo De Feyter PJ, Meijboom WB, Weustink A, Van Mieghem C, Mollet NR, Vourvouri E, Nieman K, Cademartiri F. Spiral multislice computed tomography coronary angiography: A current status report. *Clin. Cardiol.* 2007;30:437-42.

31. Dewey M, Teige F, Schnapauff D, Laule M, Borges AC, Wernecke KD, Schink T, Baumann G, Rutsch W, Rogalla P, Taupitz M, Hamm B. Noninvasive detection of coronary artery stenoses with multislice computed tomography or magnetic resonance imaging. *Ann Intern Med* 2006;145:407–15.

32. Di Carli MF&Hachamovitch R. New technology for noninvasive evaluation of coronary artery disease, *Circulation*; 2007;115:1464–80.

33. Di Carli MF, Dorbala S, Meserve J, El Fakhri G, Sitek A, Moore SC. Clinical myocardial perfusion PET/CT. *Journal of Nuclear Medicine* 2007;48:783-93.

34. Di Carli MF&Dorbala S. Cardiac PET-CT. *Journal of Thoracic Imaging* 2007;22:101-6.

35. Di Tanna GL, Berti E, Stivanello E, Cademartiri F, Achenbach S, Camerlingo MD,Grilli R. Informative value of clinical research on multislice computed tomography in the diagnosis of coronary artery disease: A systematic review. *Int J Cardiol* 2008;130:386-404.

36. Dries DL, Exner DV, Gersh BJ, Domanski MJ, Waclawiw MA, Stevenson LW. Atrial fibrillation is associated with an increased risk for mortality and heart failure progression in patients with asymptomatic and symptomatic left ventricular systolic dysfunction: a retrospective analysis of the SOLVD trials. Studies of Left Ventricular Dysfunction. *J Am Coll Cardiol* 1998;32:695-703.

37. Einstein AJ, Moser KW, Thompson RC, Cerqueira MD, Henzlova MJ. Radiation dose to patients from cardiac diagnostic imaging. *Circulation* 2007;116:1290-305.

38. El Fakhri G, Kardan A, Sitek A, Dorbala S, Abi-Hatem N, Lahoud Y, Fischman A, Coughlan M, Yasuda T, Di Carli MF. Reproducibility and accuracy of quantitative myocardial blood flow assessment with (82)Rb PET: comparison with (13)N-ammonia PET. *J Nucl Med.* 2009;50:1062-71.

39. Fei X, Du X, Li P, Liao J, Shen Y, Li K. Effect of dose-reduced scan protocols on cardiac coronary image quality with 64-row MDCT: a cardiac phantom study. *Eur J Radiol.* 2008;67::85-91.

40. Ferencik M, Nomura CH, Maurovich-Horvat P, Hoffmann U, Pena AJ, Cury RC, Abbara S, Nieman K, Fatima U, Achenbach S, Brady TJ. Quantitative parameters of image quality in 64-slice computed tomography angiography of the coronary arteries. *Eur J Radiol* 2006;57:373-9.

41. Flegel KM, Shipley MJ, Rose G. Risk of stroke in non-rheumatic atrial fibrillation. *Lancet* 1987;1:526-9.

42. Fox K, Garcia MA, Ardissino D, Buszman P, Camici PG, Crea F, Daly C, De BG, Hjemdahl P, Lopez-Sendon J, Marco J, Morais J, Pepper J, Sechtem U, Simoons M, Thygesen K, Priori SG, Blanc JJ, Budaj A, Camm J, Dean V, Deckers J, Dickstein K, Lekakis J, McGregor K, Metra M, Morais J, Osterspey A, Tamargo J, Zamorano JL. Guidelines on the management of stable angina pectoris: executive summary: The Task Force on the Management of Stable Angina Pectoris of the European Society of Cardiology. *Eur Heart J* 2006;27:1341-81.

43. Fuster V, Ryden LE, Cannom DS, Crijns HJ, Curtis AB, Ellenbogen KA, Halperin JL, Le Heuzey JY, Kay GN, Lowe JE, Olsson SB, Prystowsky EN, Tamargo JL, Wann S, Smith SC, Jr., Jacobs AK, Adams CD, Anderson JL, Antman EM, Halperin JL, Hunt SA, Nishimura R, Ornato JP, Page RL, Riegel B, Priori SG, Blanc JJ, Budaj A, Camm AJ, Dean V, Deckers JW, Despres C, Dickstein K, Lekakis J, McGregor K, Metra M, Morais J, Osterspey A, Tamargo JL, Zamorano JL. ACC/AHA/ESC 2006 Guidelines for the Management of Patients with Atrial Fibrillation: a report of the American College of Cardiology/American Heart Association Task Force on Practice Guidelines and the European Society of Cardiology Committee for Practice Guidelines (Writing Committee to Revise the 2001 Guidelines for the Management of Patients With Atrial Fibrillation): developed in collaboration with the European Heart Rhythm Association and the Heart Rhythm Society. *Circulation* 2006;114:e257-e354.

44. Gaemperli O, Schepis T, Koepfli P, Valenta I, Soyka J, Leschka S, Desbiolles L, Husmann L, Alkadhi H, Kaufmann PA. Accuracy of 64-slice CT angiography for the detection of functionally relevant coronary stenoses as assessed with myocardial perfusion SPECT. *Eur J Nucl Med Mol Imaging* 2007;34:1162-71.

45. Grosse C, Globits S, Hergan K. Forty-slice spiral computed tomography of the coronary arteries: assessment of image quality and diagnostic accuracy in a non-selected patient population. *Acta Radiol* 2007;48:36-44.

46. Hack SN, Eichling JO, Bergmann SR, Welch MJ. Sobel BE. External quantification of myocardial perfusion by exponential infusion of positron-emitting radionuclides. *J Clin Invest* 1980;66:918.

47. Hausleiter J, Meyer T, Hadamitzky M, Huber E, Zankl M, Martinoff S, Kastrati A, Schömig A.. Radiation dose estimates from cardiac multislice computed tomography in daily practice: impact of different scanning protocols on effective dose estimates. *Circulation* 2006;113:1305-10.

48. Hecht HS, Bhatti T. How much calcium is too much calcium for coronary computerized tomographic angiography? *J Cardiovasc Comput Tomogr.* 2008;2:183-7.

49. Heller GV, Calnon D, Dorbala S. Recent advances in cardiac PET and PET/CT myocardial perfusion imaging. *J Nucl Cardiol.* 2009;16:962-9.

50. Herrero P, Markham J, Shelton ME, Weinheimer CJ, Bergmann SR. Noninvasive quantification of regional myocardial perfusion PET and myocardial perfusion with rubidium-82 and positron emission tomography. Exploration of a mathematical model. *Circulation* 1990;82:1377-86.

51. Herzog BA, Husmann L, Burkhard N, Gaemperli O, Valenta I, Tatsugami F, Wyss CA, Landmesser U, Kaufmann PA. Accuracy of low-dose computed tomography coronary angiography using prospective electrocardiogram-triggering: first clinical experience. *Eur Heart J.* 2008;29:3037-42.

52. Herzog BA, Husmann L, Burkhard N, Valenta I, Gaemperli O, Tatsugami F, Wyss CA, Landmesser U, Kaufmann PA. Low-dose CT coronary angiography using prospective ECG-triggering: impact of mean heart rate and heart rate variability on image quality. *Acad Radiol.* 2009;16:15-21.

53. Hounsfield GN. Computerized transverse axial scanning (tomography) 1. Description of system, *Br J Radiol* 1973;46:1016-22.

54. Hsieh J, Londt J, Vass M, Li J, Tang X, Okerlund D. Step-and-shoot data acquisition and reconstruction for cardiac x-ray computed tomography. *Med.Phys* 2006;33:4236-48.

55. Huisman MC, Higuchi T, Reder S, Nekolla SG, Poethko T, Wester HJ, Ziegler SI, Casebier DS, Robinson SP, Schwaiger M. Initial characterization of an 18F-labeled myocardial perfusion tracer. *J Nucl Med* 2008;49:630-6.

56. Hurwitz LM, Reiman RE, Yoshizumi TT, Goodman PC, Toncheva G, Nguyen G, Lowry, C. Radiation Dose from Contemporary Cardiothoracic Multidetector CT Protocols with an Anthropomorphic Female Phantom: Implications for Cancer Induction. *Radiology* 2007;245:742-50.

57. Husmann L, Valenta I, Gaemperli O, Adda O, Treyer V, Wyss CA, Veit-Haibach P, Tatsugami F, von Schulthess GK, Kaufmann PA. Feasibility of low-dose coronary CT angiography: first experience with prospective ECG-gating. *Eur Heart J* 2008;29:191-7.

58. Hutchins GD, Schwaiger M, Rosenspire KC, Krivokapich J, Schelbert H, Kuhl DE. Noninvasive quantification of regional blood flow in the human heart using N-13 ammonia and dynamic positron emission tomographic imaging. *J Am Coll Cardiol* 1990;15:1032-42.

59. Iida H, Kanno I, Takahashi A, Miura S, Murakami M, Takahashi K, Ono Y, Shishido F, Inugami A, Tomura N. Measurement of absolute myocardial blood flow with H2 15O and dynamic positron-

emission tomography. Strategy for quantification in relation to the partial-volume effect. *Circulation* 1988;78:104-15.

60. Jacobs JE, Boxt LM, Desjardins B, Fishman EK, Larson PA, Schoepf J. ACR practice guideline for the performance and interpretation of cardiac computed tomography (CT*). J Am Coll Radiol* 2006;3:677–85.

61. Janne d'Othée B, Siebert U, Cury R, Jadvar H, Dunn EJ, Hoffmann U. A systematic review on diagnostic accuracy of CT based detection of significant coronary artery disease. *Eur J Radiol.* 2008;65:449–61.

62. Kalender WA, Wolf H, Siess C, et al. Dose reduction in CT by on-line tube current control: principles and validation on phantoms and cadavers. *Eur Radiol* 1999;9:323-8.

63. Kannel WB, McGee D, Gordon T. A general cardiovascular risk profile: the Framingham study. *Am J Cardiol* 1976;38:46–51.

64. Kannel WB&McGee DL. Diabetes and cardiovascular disease. The Framingham study. *JAMA* 1979;241:2035–8.

65. Kannel WB, Abbott RD, Savage DD, McNamara PM. Epidemiologic features of chronic atrial fibrillation: the Framingham study. *N Engl J Med* 1982;306:1018-22.

66. Kannel WB, Abbott RD, Savage DD, McNamara PM. Coronary heart disease and atrial fibrillation: the Framingham Study. *Am Heart J* 1983;106:389-96.

67. Kaufmann PA, Gnecchi-Ruscone T, Yap JT, Rimoldi O, Camici PG. Assessment of the reproducibility of baseline and hyperemic myocardial blood flow measurements with 15O-labeled water and PET. *J Nucl Med.* 1999;40:1848-56.

68. Kaufmann PA& Di Carli MF. Hybrid SPECT/CT and PET/CT imaging: the next step in noninvasive cardiac imaging. *Semin Nucl Med.* 2009;39:341-7.

69. Kaufmann PA. Cardiac hybrid imaging: state-of-the-art. *Ann Nucl Med.* 2009;23:325-31.

70. Knabb RM, Fox KA, Sobel BE, Bergmann SR. Characterization of the functional significance of subcritical coronary stenoses with H(2)15O and positron-emission tomography. *Circulation* 1985;71:1271-8.

71. Knuuti J, Kajander S, Mäki M, Ukkonen H. Quantification of myocardial blood flow will reform the detection of CAD. *J Nucl Cardiol.* 2009a;16:497-506.

72. Knuuti J. Integrated positron emission tomography/computed tomography (PET/CT) in coronary disease. *Heart.* 2009b;95:1457-63.

73. Krahn AD, Manfreda J, Tate RB, Mathewson FA, Cuddy TE. The natural history of atrial fibrillation: incidence, risk factors, and prognosis in the Manitoba Follow-Up Study. *Am J Med* 1995;98:476-84.

74. Laine H, Raitakari OT, Niinikoski H, Pitkänen OP, Iida H, Viikari J, Nuutila P, Knuuti J. Early impairment of coronary flow reserve in young men with borderline hypertension. *J Am Coll Cardiol.* 1998;32:147-53.

75. Leschka S, Alkadhi H, Plass A, Desbiolles L, Grünenfelder J, Marincek B, Wildermuth S. Accuracy of MSCT coronary angiography with 64-slice technology: first experience. *Eur Heart J* 2005;26:1482-7.

76. Leschka S, Husmann L, Desbiolles LM, et al. Optimal image reconstruction intervals for non-invasive coronary angiography with 64-slice CT. *Eur Radiol* 2006;16:1964-72.

77. Leschka S, Stolzmann P, Desbiolles L, Baumueller S, Goetti R, Schertler T,Scheffel H, Plass A, Falk V, Feuchtner G, Marincek B, Alkadhi H. Diagnostic accuracy of high-pitch dual-source CT for the assessment of coronary stenoses: first experience. *Eur Radiol.* 2009;19:2896-903.

78. Leschka S, Stolzmann P, Schmid FT, Scheffel H, Stinn B, Marincek B, Alkadhi H,Wildermuth S. Low kilovoltage cardiac dual-source CT: attenuation, noise, and radiation dose. *Eur Radiol.* 2008;18:1809-17.

79. Lip GY, Beevers DG. ABC of atrial fibrillation. History, epidemiology, and importance of atrial fibrillation. *BMJ* 1995;311:1361-3.

80. Lodge MA, Bengel FM. Methodology for quantifying absolute myocardial perfusion with PET and SPECT. *Curr Cardiol Rep.* 2007;9:121-8.

81. Madar I, Ravert HT, Du Y, Hilton J, Volokh L, Dannals RF, Frost JJ, Hare JM. Characterization of uptake of the new PET imaging compound 18F-fluorobenzyl triphenyl phosphonium in dog myocardium. *J Nucl Med* 2006;47:1359-66.

82. McCollough CH, Primak AN, Saba O, Bruder H, Stierstorfer K, Raupach R, Suess C, Schmidt B, Ohnesorge BM, Flohr TG. Dose performance of a 64-channel dual-source CT scanner. *Radiology* 2007;243:775-84.

83. Meijboom WB, Van Mieghem CA, van Pelt N, Weustink A, Pugliese F, Mollet NR, Boersma E, Regar E, van Geuns RJ, de Jaegere PJ, Serruys PW, Krestin GP, de Feyter PJ. Comprehensive assessment of coronary artery stenoses - Computed tomography coronary angiography versus conventional coronary angiography and correlation with fractional flow reserve in patients with stable angina. *Journal of the American College of Cardiology* 2008;52:636-43.

84. Miller JM, Dewey M, Vavere AL, Rochitte CE, Niinuma H, Arbab-Zadeh A, Paul N, Hoe J, de Roos A, Yoshioka K, Lemos PA, Bush DE, Lardo

AC, Texter J, Brinker J, Cox C, Clouse ME, Lima JA. Coronary CT angiography using 64 detector rows: methods and design of the multi-centre trial CORE-64. *Eur Radiol* 2009;19:816-28.

85. Mir-Akbari H, Ripsweden J, Jensen J, Pichler P, Sylvén C, Cederlund K, Rück A. Limitations of 64-detector-row computed tomography coronary angiography: calcium and motion but not short experience. *Acta Radiol* 2009; 50:174-80.

86. Morin RL, Gerber TC, McCollough CH. Radiation dose in computed tomography of the heart. *Circulation* 2003;107:917–22.

87. Morrow K, Morris CK, Froelicher VF, Hideg A, Hunter D, Johnson E, Kawaguchi T, Lehmann K, Ribisl PM, Thomas R, Ueshima K, Froelicher E, Wallis J. Prediction of cardiovascular death in men undergoing noninvasive evaluation for coronary artery disease. *Ann Intern Med.* 1993;118:689-95.

88. Mowatt G, Cook JA, Hillis GS, Walker S, Fraser C, Jia X, Waugh N. 64-Slice computed tomography angiography in the diagnosis and assessment of coronary artery disease: systematic review and meta-analysis. *Heart* 2008;94:1386-93.

89. Muzik O, Beanlands RS, Hutchins GD, Mangner TJ, Nguyen N, Schwaiger M. Validation of nitrogen-13-ammonia tracer kinetic model for quantification of myocardial blood flow using PET. *J Nucl Med* 1993;34:83-91.

90. Muzik O, Duvernoy C, Beanlands RS, Sawada S, Dayanikli F, Wolfe ER Jr, Schwaiger M. Assessment of diagnostic performance of quantitative flow measurements in normal subjects and patients with angiographically documented coronary artery disease by means of nitrogen-13 ammonia and positron emission tomography. *J Am Coll Cardiol.* 1998;31:534-40.

91. Myers RH, Kiely DK, Cupples LA, *et al*.. Parental history is an independent risk factor for coronary artery disease: the Framingham study. *Am Heart J* 1990;120:963–9.

92. Nandalur KR, Dwamena BA, Choudhri AF, Nandalur MR, Carlos RC. Diagnostic performance of stress cardiac magnetic resonance imaging in the detection of coronary artery disease: a meta-analysis. *J Am Coll Cardiol* 2007;50:1343-53.

93. Nandalur KR, Dwamena BA, Choudhri AF, Nandalur SR, Reddy P, Carlos RC. Diagnostic performance of positron emission tomography in the detection of coronary artery disease: a meta-analysis. *Acad Radiol* 2008;15:444-51.

94. Nickoloff EL, Alderson PO. A comparative study of thoracic radiation doses from 64-slice cardiac CT. *The British Journal of Radiology* 2007;80:537-44.

95. Pandit-Taskar N, Grewal RK, Strauss HW. Cardiovascular system. In: Christian PE, Waterstram-Rich KM, eds. Nuclear medicine and PET/CT technology and techniques. St. Louis: Mosby Elsevier; 2007. pp. 479-512.

96. Pannu HK, Jacobs JE, Lai S, Fishman EK. Coronary CT angiography with 64-MDCT: assessment of vessel visibility. *AJR* 2006;187:119 -26.

97. Parkash R, deKemp RA, Ruddy TD, Kitsikis A, Hart R, Beauchesne L, Williams K, Davies RA, Labinaz M, Beanlands RS. Potential utility of rubidium 82 PET quantification in patients with 3-vessel coronary artery disease. *J Nucl Cardiol.* 2004;11:440-9.

98. Paul J-F & Abada HT. Strategies for reduction of radiation dose in cardiac multislice CT. *Eur Radiol* 2007;17:2028-37.

99. Pijls NH. Optimum guidance of complex PCI by coronary pressure measurement. *Heart* 2004;90:1085-93.

100. Pitkänen OP, Nuutila P, Raitakari OT, Porkka K, Iida H, Nuotio I, Rönnemaa T, Viikari J, Taskinen MR, Ehnholm C, Knuuti J. Coronary flow reserve in young men with familial combined hyperlipidemia. *Circulation*. 1999;99:1678-84.

101. Plössl K, Chandra R, Qu W, Lieberman BP, Kung MP, Zhou R, Huang B, Kung HF.. A novel gallium bisaminothiolate complex as a myocardial perfusion imaging agent. *Nucl Med Biol* 2008;35:83-90.

102. Pontone G, Andreini D, Bartorelli AL, Cortinovis S, Mushtaq S, Bertella E, Annoni A, Formenti A, Nobili E, Trabattoni D, Montorsi P, Ballerini G, Agostoni P, Pepi M. Diagnostic accuracy of coronary computed tomography angiography: a comparison between prospective and retrospective electrocardiogram triggering. *J Am Coll Cardiol.* 2009;54:346-55.

103. Primak AN, McCollough CH, Bruesewitz MR, Zhang J, Fletcher JG. Relationship between noise, dose, and pitch in cardiac multi-detector row CT. *Radiographics* 2006;26:1785-94.

104. Psaty BM, Manolio TA, Kuller LH, Kronmal RA, Cushman M, Fried LP,White R, Furberg CD, Rautaharju PM. Incidence of and risk factors for atrial fibrillation in older adults. *Circulation* 1997;96:2455-61.

105. Pugliese F, Mollet NR, Runza G, van Mieghem C, Meijboom WB, Malagutti P, Baks T, Krestin GP, deFeyter PJ, Cademartiri F. Diagnostic accuracy of non-invasive 64-slice CT coronary angiography in patients with stable angina pectoris. *Eur Radiol* 2006;16:575-82.

106. Raff GL, Gallagher MJ, O'Neill WW, Goldstein JA. Diagnostic accuracy of noninvasive coronary angiography using 64-slice spiral computed tomography. *J Am Coll Cardiol* 2005;46:552-7.

107. Raff GL, Chinnaiyan KM, Share DA, Goraya TY, Kazerooni EA, Moscucci M, Gentry RE,

Abidov A. Advanced Cardiovascular Imaging Consortium Co-Investigators. Radiation dose from cardiac computed tomography before and after implementation of radiation dose-reduction techniques. *JAMA* 2009;301:2340-8.

108. Rogalla P, Kloeters C, Hein PA. CT Technology Overview. 64-Slice and Beyond. *Radiol Clin North Am* 2009;*47:1-11*.

109. Rubin GD. MDCT and Data Explosion. Current Technologies and Directions for Future Development in managing the Information Overload. In: Marchal G, Vogl TJ, Heiken JP. Rubin GD. *Multidetector-row computed tomography: scanning and contrast protocols. Springer* 2005; 113.

110. Sampson UK, Dorbala S, Limaye A, Kwong R, Di Carli MF. Diagnostic accuracy of rubidium-82 myocardial perfusion imaging with hybrid positron emission tomography/computed tomography in the detection of coronary artery disease. *J Am Coll Cardiol.* 2007;49:1052-8.

111. Scheffel H, Alkadhi H, Leschka S, Plass A, Desbiolles L, Guber I, Krauss T, Gruenenfelder J, Genoni M, Luescher TF, Marincek B, Stolzmann P. Low-dose CT coronary angiography in the step-and-shoot mode: diagnostic performance. *Heart.* 2008;94:1132-7.

112. Schenker MP, Dorbala S, Hong EC, Rybicki FJ, Hachamovitch R, Kwong RY, Di Carli MF. Interrelation of coronary calcification, myocardial ischemia, and outcomes in patients with intermediate likelihood of coronary artery disease: a combined positron emission tomography/computed tomography study. *Circulation* 2008;117:1693-700.

113. Schoenhagen P. Back to the future: coronary CT angiography using prospective ECG triggering. *Eur Heart J.* 2008;29:153-4.

114. Schoonderwoerd BA, Van Gelder I, Crijns HJ. Left ventricular ischemia due to coronary stenosis as an unexpected treatable cause of paroxysmal atrial fibrillation. *J Cardiovasc Electrophysiol* 1999;10:224-8.

115. Schuijf JD, Bax JJ, Shaw LJ, de Roos A, Lamb HJ, van der Wall EE, Wijns W. Meta-analysis of comparative diagnostic performance of magnetic resonance imaging and multislice computed tomography for noninvasive coronary angiography. *Am Heart J* 2006;151:404–11.

116. Schwitter J, Wacker CM, van Rossum AC, Lombardi M, Al-Saadi N, Ahlstrom H, Dill T, Larsson HB, Flamm SD, Marquardt M, Johansson L. MR-IMPACT: comparison of perfusion-cardiac magnetic resonance with single-photon emission computed tomography for the detection of coronary artery disease in a multicentre, multivendor, randomized trial. *Eur Heart J* 2008;29:480-9.

117. Stein PD, Beemath A, Kayali F, Skaf E, Sanchez J, Olson RE. Multidetector computed tomography for the diagnosis of coronary artery disease: a systematic review. *Am J Med* 2006;119:203–16.

118. Stolzmann P, Scheffel H, Schertler T, Frauenfelder T, Leschka S, Husmann L, Flohr TG, Marincek B, Kaufmann PA, Alkadhi H.. Radiation dose estimates in dual-source computed tomography coronary angiography. *Eur Radiol* 2008;18:592-9.

119. Sun Z, Lin C, Davidson R, Dong C, Liao Y. Diagnostic value of 64-slice CT angiography in coronary artery disease: A systematic review. *Eur J Radiol.* 2008; 67:78-84.

120. Tonino PA, De Bruyne B, Pijls NH, Siebert U, Ikeno F, van' t Veer M, Klauss V, Manoharan G, Engstrøm T, Oldroyd KG, Ver Lee PN, MacCarthy PA, Fearon WF; FAME Study Investigators. Fractional flow reserve versus angiography for guiding percutaneous coronary intervention. *N Engl J Med* 2009;360:213-24.

121. Townsend DW, Beyer T. A combined PET/CT scanner: the path to true image fusion. *Br J Radiol.* 2002;75 Spec No:S24-30.

122. Uren NG, Melin JA, De Bruyne B, Wijns W, Baudhuin T, Camici PG. Relation between myocardial blood flow and the severity of coronary-artery stenosis. *N Engl J Med.* 1994;330:1782-8.

123. Vanhoenacker PK, Heijenbrok-Kal MH, Van Heste R, Decramer I, Van Hoe LR, Wijns W, Hunink MG. Diagnostic performance of multidetector CT angiography for assessment of coronary artery disease: Meta-analysis. *Radiology* 2007;244:419-28.

124. Wang G, Yu H, De Man B. An outlook on x-ray CT research and development. *Med Phys.* 2008;35:1051-64.

125. Wilson PW, D'Agostino RB, Levy D, Belanger AM, Silbershatz H, Kannel WB. Prediction of coronary heart disease using risk factor categories. *Circulation* 1998;97:1837-47.

126. Wintersperger BJ, Nikolaou K, von Ziegler F, Johnson T, Rist C, Leber A, Flohr T, Knez A, Reiser MF, Becker CR. Image quality, motion artifacts, and reconstruction timing of 64-slice coronary computed tomography angiography with 0.33-second rotation speed. *Invest Radiol* 2006;41:436-42.

127. Yoshinaga K, Chow BJ, Williams K, Chen L, deKemp RA, Garrard L, Lok-Tin Szeto A, Aung M, Davies RA, Ruddy TD, Beanlands RS. What is the prognostic value of myocardial perfusion imaging using rubidium-82 positron emission tomography? J *Am Coll Cardiol.* 2006;5;48:1029-39.